On Concentrated Surface Loads and Green's functions in the Toupin-Mindlin theory of Strain-Gradient Elasticity

P.A. Gourgiotis [1*], Th. Zisis [2], H.G. Georgiadis [2,3]

[1] *School of Engineering & Computing Sciences, Durham University, South Road, Durham, DH1 3LE, U.K.*

[2] *Mechanics Division, National Technical University of Athens, Zographou, GR-15773, Greece*

[3] *Office of Theoretical and Applied Mechanics, Academy of Athens, Greece*

Abstract. The two-dimensional Green's functions are derived for the half-plane in the context of the complete Toupin-Mindlin theory of isotropic strain-gradient elasticity. Two types of Green's functions exist for a concentrated force and a concentrated force dipole acting upon the surface of a traction-free half-plane. Our purpose is to examine the possible deviations from the predictions of classical theory of elasticity as well as from the simplified strain-gradient theory, which is frequently utilized in the last decade for the solution of boundary value problems. Of special importance is the behavior of the new solutions near to the point of application of the loads where pathological singularities and discontinuities exist in the classical solutions. The boundary value problems are attacked with the aid of the Fourier transform and exact full-field solutions are provided. Our results indicate that in all cases the displacement field is bounded and continuous at the point of application of the concentrated loads. The new solutions show therefore a more natural material response. For the concentrated force problem, both displacements and strains are found to be bounded, whereas the strain-gradients exhibit a logarithmic singularity. Thus, in marked contrast with the classical elasticity solution, a finite strain energy is contained within any finite portion of the body. On the other hand, in the case of the concentrated dipole force, the strains are logarithmically singular and the strain gradients exhibit a Cauchy type singularity. The nature of the boundary conditions in strain-gradient elasticity is highlighted through the solution of the pertinent boundary value problems. Finally, based on our analytical solution, the role of edge forces in strain-gradient elasticity is elucidated employing simple equilibrium considerations.

Keywords: microstructure; strain-gradient theory; half-plane; force dipole, edge forces, bounded energy, true boundary conditions.

[*] Corresponding author: Panos Gourgiotis. panagiotis.gourgiotis@durham.ac.uk

1. Introduction

In the present work, the two-dimensional Green's functions for a body in the form of a half-plane are derived in the context of the complete Toupin-Mindlin theory of isotropic strain-gradient elasticity (Toupin, 1962; Mindlin, 1964). Two types of Green's functions exist for a concentrated force and a concentrated force dipole acting upon the surface of a traction-free half-plane. The first case corresponds to the well-known Flamant problem which is one of the most celebrated problems in the classical linear elastostatic theory finding applications in contact mechanics, geomechanics, and tribology (Johnson, 1987; Goryacheva 2013; Podio-Guidugli and Favata, 2014). The second case regarding the concentrated force dipole has no direct counterpart in the frame of the classical elasticity theory.

The Toupin-Mindlin's theory assumes that each material particle has three degrees of freedom (that is the displacement components as in the classical theory), the micro-density coincides with the macro-density, and the strain energy density depends not only upon the strain but also upon the strain gradient (a third order tensor). In the isotropic case, the full constitutive relations involve *five* microstructural parameters (these constants are additional to the standard Lame constants to characterize the material response), providing thus a more detailed description of microstructured materials as compared to the *simplified* strain-gradient elasticity (including only the additional material parameter - the so-called gradient coefficient) or other generalized continuum theories – like the couple stress (constrained Cosserat) theory or the micropolar (unconstrained Cosserat) theory. A recent study by Bacca et al. (2013) provides an account of the determination of the five gradient moduli via homogenization of heterogeneous materials. Moreover, Shodja et al. (2013) utilizing ab initio DFT calculations evaluated the characteristic material lengths of the complete Toupin-Mindlin strain-gradient elasticity theory for several FCC and BCC metal crystals. More recently, Po et al. (2017) based on atomistic calculations provided estimates of the length scale parameters in gradient elasticity for many anisotropic structures. Finally, strain gradient effects, even though difficult to be measured, have been experimentally observed in rigid polyurethane and polymethacrylimide foams (Anderson and Lakes, 1994).

Although the simplified strain-gradient elasticity has been extensively used in the last two decades for the solution of various boundary value problems (see e.g. Vardoulakis and Georgiadis, 1997; Georgiadis et al., 2000; Papargyri-Beskou et al., 2003; Vardoulakis and Giannakopoulos, 2006; Gao and Ma, 2009; Gourgiotis and Georgiadis, 2009; Aravas and Giannakopoulos, 2009; Filopoulos et al., 2010; Gao and Zhou, 2013; Rosi et al. 2014; Li and Wei, 2015; Papathanasiou et al. 2016 and references therein), the complete Toupin-Mindlin theory of strain-gradient elasticity, due to its complexity, has not been adequately explored. Indeed, there exist only a few works in the literature that

employ the complete Toupin-Mindlin theory, most of them treating stress concentration problems (Cook and Weitsman, 1966; Day and Weitsman, 1966; Weitsman, 1966; Hazen and Weitsman, 1968; Adler, 1969; Eshel and Rosenfeld 1970; Lardner, 1970; Eshel and Rosenfeld, 1973; Lardner, 1971; Eshel and Rosenfeld 1975) and recently crack and wave propagation problems (Sciarra and Vidoli, 2013; Gourgiotis and Georgiadis, 2015; Rosi and Auffray, 2016; Lazar, 2016; Reda et al., 2017).

As is well known, the solution of the Flamant problem in the context of classical elasticity predicts a logarithmic singularity for the displacement field at the point of application of the load (Love, 1944), thus violating the basic premise of linearized (i.e. infinitesimal) elasticity. In fact, unbounded displacements occur at the point of application of the load, no matter how small the load intensity is. It is obvious, therefore, that the classical elasticity solution does not reflect (to some extent) the actual situation. To remedy the aforementioned deficiency, various generalized continuum theories have been employed for the solution of the problem. In particular, the Flamant problem was initially solved asymptotically in the context of the couple-stress theory by Muki and Sternberg (1965), and by Cowin (1969) and Dyszlewicz and Matysiak (1973) in the framework of micropolar theory. In the context of non-local elasticity, the problem was treated first by Nowinski (1986) and later by Wang (1990). In all of these cases, however, the singularity in the displacement field was *not* eliminated. More recently, in the context of the *simplified* strain-gradient elasticity, the Flamant problem was solved by Exadaktylos (1999), Polyzos et al. (2003), Lazar and Maugin (2006), and by Georgiadis and Anagnostou (2008). In the latter study, the exact boundary conditions were used showing that even the simplified gradient theory predicts *bounded* and *continuous* displacements at the point of application of the load and, therefore, 'corrects' (in a boundary-layer sense) the classical solution. Finally, mention should be made to the work of Lardner (1970) that the present authors encountered recently. In this work, the complete Toupin-Mindlin theory is employed to treat the Flamant problem through the use of Lamé potentials. However, only rudimentary asymptotic results are presented for the stresses at the point of application of the load while the effect of the gradient parameters is not discussed. Moreover, as Sternberg (1960) pointed out, in static problems the Lamé potentials do not constitute a complete representation of solutions of elastic equilibrium (see also Eringen and Suhubi, 1975).

The aim of the present study is to derive the half-plane Green's functions of the complete Toupin-Mindlin theory under plane-strain conditions and examine the possible deviations from the predictions of classical theory of elasticity but also from the frequently used simplified strain-gradient theory. Of special importance is the behavior of the new solutions near to the point of application of the loads where pathological singularities and discontinuities exist in the classical solution. The boundary value problems are attacked with the aid of the Fourier transform and exact full-field solutions are provided. It is shown that in all cases the displacement field is bounded and continuous in the

vicinity of the point of application of the concentrated loads. The new solutions show therefore a more natural material response. In particular, for the Flamant problem both displacement and strains are bounded, whereas the strain-gradients exhibit a logarithmic singularity. Thus, in marked contrast with the classical elasticity solution, a finite strain energy is contained within any finite portion of the body. On the other hand, in the case of the concentrated force dipoles, the strains are logarithmically singular and the strain gradients exhibit a Cauchy type singularity.

The contents of our paper are as follows: In Section 2, we summarize the basic equations of the Form II of Toupin-Mindlin strain-gradient theory and examine the conditions for positive definiteness of the strain-energy density. Next, in Section 3, we recall certain pertinent elements of the plane-strain theory with which we are concerned. In Section 4, the Green's functions of the Toupin-Mindlin strain-gradient theory are analytically derived using a Fourier transform analysis. The role of edge forces in strain-gradient elasticity is elucidated in Section 5. Numerical results regarding the displacement and strain fields are presented in Section 6.

2. Fundamentals of the Toupin-Mindlin strain gradient elasticity theory

The basic equations of the Toupin-Mindlin strain-gradient elasticity theory (Toupin, 1962; Mindlin, 1964) of homogeneous elastic solids will be now briefly presented. An interesting and concise exposition of the theory was given by Mindlin and Eshel (1968), Eshel and Rosenfeld (1970), and more recently by Gourgiotis and Georgiadis (2015) for the dynamical case including micro-inertia effects. In what follows, we confine our attention to the equilibrium case and neglect the contribution of body forces and body dipoles. In addition, all equations are referred to a rectangular Cartesian coordinate system, $\partial_p(\ ) \equiv \partial(\ )/\partial x_p$ where the Latin indices span the range (1,2,3), and indicial notation and summation convention is used throughout.

The point of departure is the strain-energy density function for an isotropic and centrosymmetric material

$$W = \frac{1}{2}\lambda\varepsilon_{pp}\varepsilon_{qq} + \mu\varepsilon_{pq}\varepsilon_{pq} + a_1\kappa_{ppk}\kappa_{kqq} + a_2\kappa_{kpp}\kappa_{kqq} + a_3\kappa_{ppk}\kappa_{qqk} + a_4\kappa_{kpq}\kappa_{kpq} + a_5\kappa_{kpq}\kappa_{qpk}\ , \tag{1}$$

where u_p is the displacement vector, $\varepsilon_{pq} = (1/2)\left(\partial_p u_q + \partial_q u_p\right) = \varepsilon_{qp}$ is the linear strain tensor, and $\kappa_{rpq} = \kappa_{rqp} = \partial_r \varepsilon_{pq}$ is the strain gradient (third order) tensor. This is the so-called Form II version of

gradient elasticity in Mindlin's terminology (Mindlin, 1964). In addition, (λ, μ) are the standard Lamé constants and a_q $(q = 1,...,5)$ are the five additional material constants (gradient parameters) having dimensions of [force]. It is worth noting that the frequently used simplified gradient elasticity is rigorously obtained from Eq. (1) by setting: $a_2 = \lambda \ell^2/2$, $a_4 = \mu \ell^2$, and $a_1 = a_3 = a_5 = 0$, where ℓ is a characteristic material length (see e.g. Georgiadis et al. 2004).

The constitutive equations of the theory assume then the following form

$$\tau_{pq} = \frac{\partial W}{\partial \varepsilon_{pq}} = \lambda \varepsilon_{kk} \delta_{pq} + 2\mu \varepsilon_{pq} \ , \tag{2}$$

$$m_{rpq} = \frac{\partial W}{\partial \kappa_{rpq}} = \frac{1}{2} a_1 \left(\delta_{rp} \kappa_{qkk} + 2\delta_{pq} \kappa_{kkr} + \delta_{qr} \kappa_{pkk} \right) + 2a_2 \delta_{pq} \kappa_{rkk}$$
$$+ a_3 \left(\delta_{rp} \kappa_{kkq} + \delta_{rq} \kappa_{kkp} \right) + 2a_4 \kappa_{rpq} + a_5 \left(\kappa_{qrp} + \kappa_{pqr} \right) \ , \tag{3}$$

where δ_{pq} is the Kronecker delta, τ_{pq} is the monopolar (Cauchy) stress tensor, and m_{rpq} is the dipolar (or double) stress tensor (a third-rank tensor) expressed in dimensions of [force][length]$^{-1}$. The dipolar stress tensor follows from the notion of dipolar forces, which are anti-parallel forces acting between the micro-media contained in the continuum with microstructure (Jaunzemis, 1967). According to Eqs. (2) and (3), the following symmetries for the monopolar and dipolar stress tensors are noticed: $\tau_{pq} = \tau_{qp}$ and $m_{rpq} = m_{rqp}$.

The equations of equilibrium and the traction boundary conditions along the boundary are derived from variational considerations using Eqs. (2) and (3). These equations read

$$\partial_p \left(\tau_{pq} - \partial_r m_{rpq} \right) = 0 \quad \text{in} \quad V \ , \tag{4}$$

$$P_q^{(n)} = n_p \left(\tau_{pq} - \partial_r m_{rpq} \right) - D_p \left(n_r m_{rpq} \right) + \left(D_k n_k \right) n_r n_p m_{rpq} \quad \text{on} \quad S \ , \tag{5}$$

$$R_q^{(n)} = n_r n_p m_{rpq} \quad \text{on} \quad S \ , \tag{6}$$

$$E_q = \left[\left[n_r k_p m_{rpq} \right] \right] \quad \text{on} \quad C \ , \tag{7}$$

where V is the region (open set) occupied by the body, S denotes the bounding surface, and C denotes every edge formed by the intersection of two portions, say S_1 and S_2 of the (closed) bounding surface S. The double brackets [[ ]] indicate the difference of the enclosed quantity as a given point

on the edge is approached from either side. Also, n_p is the outward unit normal to the boundary, s_q is the unit tangent vector to the curve C, and the vector $\mathbf{k}$ is defined as $k_q = e_{qrp}s_r n_p$. Moreover, $D_p(\ ) \equiv \partial_p(\ ) - n_p D(\ )$ is the surface gradient operator and $D(\ ) \equiv n_p \partial_p(\ )$ is the normal gradient operator.

As Bleustein (1967) points out, the auxiliary force traction $P_q^{(n)}$, dipole traction $R_q^{(n)}$, and edge force E_q are related with the *true* force traction $t_q^{(n)}$ and the *true* dipole-force traction $T_{pq}^{(n)}$ through the relations

$$P_q^{(n)} \equiv t_q^{(n)} + \left(D_r n_r\right) n_p T_{pq}^{(n)} - D_p T_{pq}^{(n)}, \tag{8}$$

$$R_q^{(n)} \equiv n_p T_{pq}^{(n)}, \tag{9}$$

$$E_q \equiv s_r \left[\left[e_{qrp} n_p T_{pq}^{(n)} \right]\right]. \tag{10}$$

Combining Eqs (5)-(7) with (8)-(10), we finally obtain

$$t_q^{(n)} - D_p T_{pq}^{(n)} = n_p \left(\tau_{pq} - \partial_k m_{kpq}\right) - D_p \left(n_k m_{kpq}\right) \quad \text{on} \quad S\ , \tag{11}$$

$$n_p T_{pq}^{(n)} = n_p n_k m_{kpq} \quad \text{on} \quad S\ , \tag{12}$$

$$\left[\!\left[k_p T_{pq}^{(n)} \right]\!\right] = \left[\!\left[n_r k_p m_{rpq} \right]\!\right] \quad \text{on} \quad C\ . \tag{13}$$

Note that in a given application one would have information about the quantities $t_q^{(n)}$ and $T_{pq}^{(n)}$ on the surface. However, as in the Kirchhoff plate theory (Timoshenko, 1959), only the quantities $t_q^{(n)} - D_p T_{pq}^{(n)}$ (analogous to the effective shear force) and $n_p T_{pq}^{(n)}$ (analogous to the bending moment) can be prescribed independently on the surface.

The kinematical boundary conditions of the theory were derived in Mindlin (1964) (see also, Grentzelou and Georgiadis, 2008), but are omitted here since these are not relevant to our specific problem.

Employing Eqs. (2) and (3) with (4), one obtains the equations of equilibrium in terms of the displacement components

$$\left(\lambda + 2\mu\right)\left(1 - \ell_1^2 \nabla^2\right) \nabla\left(\nabla \cdot \mathbf{u}\right) - \mu\left(1 - \ell_2^2 \nabla^2\right) \nabla \times \nabla \times \mathbf{u} = \mathbf{0}\ , \tag{14}$$

where $\nabla^2(\ )$ is the Laplace operator, and (ℓ_1, ℓ_2) are two characteristic material lengths, defined as

$$\ell_1^2 = \frac{2(a_1 + a_2 + a_3 + a_4 + a_5)}{\lambda + 2\mu}\ , \quad \ell_2^2 = \frac{(a_3 + 2a_4 + a_5)}{2\mu}\ . \tag{15}$$

In the limit $(\ell_1, \ell_2) \to 0$, the Navier-Cauchy equations of classical linear isotropic elasticity are recovered from (14). Note that in the simplified gradient elasticity theory: $\ell_1 = \ell_2 = \ell$. The fact that the material lengths (ℓ_1, ℓ_2) multiply the higher-order term reveals the *singular-perturbation* character of the strain-gradient theory and the emergence of associated *boundary-layer* effects.

Finally, the restriction of positive definiteness (PD) of the strain energy density W requires the following inequalities for the material constants (Gourgiotis and Georgiadis, 2015)

$$\begin{aligned}
&(3\lambda + 2\mu) > 0\ , \quad \mu > 0\ , \\
&\ell_1^2 > 0\ , \quad \ell_2^2 > 0\ , \quad a_4 > 0\ , \quad a_4 + a_5 > 0\ , \quad 2a_4 - a_5 > 0\ , \\
&b_1 > 0\ , \ b_2 > 0\ , \quad 2b_1 b_2 - 5(a_1 + 4a_2 - 2a_3)^2 > 0\ ,
\end{aligned} \tag{16}$$

where

$$b_1 = -4a_1 + 8a_2 + 2a_3 + 6a_4 - 3a_5 \quad \text{and} \quad b_2 = 5(a_1 + a_2 + a_3) + 3(a_4 + a_5)\ . \tag{17}$$

Note that combining the above inequalities we further obtain: $10a_3 + 6a_4 + a_5 > 0$. The latter inequality plays an important role in antiplane problems in strain-gradient elasticity (Gourgiotis and Georgiadis, 2015).

3. Basic equations under plane-strain conditions

For a body that occupies a domain in the (x, y)-plane under conditions of plane strain, the displacement field assumes the following general form:

$$u_x \equiv u_x(x, y) \neq 0, \quad u_y \equiv u_y(x, y) \neq 0\ , \ \ u_z(x, y) = 0 \tag{18}$$

where the z-axis is perpendicular to the (x,y)-plane. Under these circumstances, the monopolar stress tensor τ_{pq} and the double-stress tensor m_{pqk} have three and six independent in-plane components, respectively, that read

$$\tau_{xx}=(\lambda+2\mu)\frac{\partial u_x}{\partial x}+\lambda\frac{\partial u_y}{\partial y},\quad \tau_{yy}=(\lambda+2\mu)\frac{\partial u_y}{\partial y}+\lambda\frac{\partial u_x}{\partial x},\quad \tau_{xy}=\mu\left(\frac{\partial u_x}{\partial y}+\frac{\partial u_y}{\partial x}\right), \tag{19}$$

$$\begin{aligned}
m_{xxx}&=2c_1\frac{\partial^2 u_x}{\partial x^2}+\left(c_1-c_3-\frac{c_4}{2}\right)\frac{\partial^2 u_x}{\partial y^2}+\left(c_1-c_3+\frac{c_4}{2}\right)\frac{\partial^2 u_y}{\partial x\partial y}\\
m_{xxy}&=\left(c_1-\frac{c_2}{2}+c_3-\frac{c_4}{2}\right)\frac{\partial^2 u_x}{\partial x\partial y}+\frac{c_2}{2}\frac{\partial^2 u_y}{\partial x^2}+\left(c_1-c_3-\frac{c_4}{2}\right)\frac{\partial^2 u_y}{\partial y^2}\\
m_{xyy}&=c_4\frac{\partial^2 u_x}{\partial x^2}+\left(c_1-c_2+c_3-\frac{c_4}{2}\right)\frac{\partial^2 u_x}{\partial y^2}+\left(-c_1+c_2+c_3+\frac{3c_4}{2}\right)\frac{\partial^2 u_y}{\partial x\partial y}\\
m_{yxx}&=\left(-c_1+c_2+c_3+\frac{3c_4}{2}\right)\frac{\partial^2 u_x}{\partial x\partial y}+\left(c_1-c_2+c_3-\frac{c_4}{2}\right)\frac{\partial^2 u_y}{\partial x^2}+c_4\frac{\partial^2 u_y}{\partial y^2}\\
m_{yyx}&=\left(c_1-c_3-\frac{c_4}{2}\right)\frac{\partial^2 u_x}{\partial x^2}+\frac{c_2}{2}\frac{\partial^2 u_x}{\partial y^2}+\left(c_1-\frac{c_2}{2}+c_3-\frac{c_4}{2}\right)\frac{\partial^2 u_y}{\partial x\partial y}\\
m_{yyy}&=\left(c_1-c_3+\frac{c_4}{2}\right)\frac{\partial^2 u_x}{\partial x\partial y}+\left(c_1-c_3-\frac{c_4}{2}\right)\frac{\partial^2 u_y}{\partial x^2}+2c_1\frac{\partial^2 u_y}{\partial y^2}\ ,
\end{aligned} \tag{20}$$

where

$$c_1=a_1+a_2+a_3+a_4+a_5,\quad c_2=a_3+2a_4+a_5,\quad c_3=a_4+a_5,\quad c_4=a_1+2a_2. \tag{21}$$

It is worth noting that although Eq. (3) suggests that all 5 gradient parameters a_q should enter the constitutive equations, in the plane-strain case only 4 of them are independent (Eshel and Rosenfeld, 1970). Moreover, the following relations hold: $c_1=(\lambda+2\mu)\ell_1^2/2$ and $c_2=2\mu\ell_2^2$.

In view of Eq. (14), the equations of equilibrium then become

$$(\lambda+2\mu)\left(1-\ell_1^2\nabla^2\right)\left(\frac{\partial^2 u_x}{\partial x^2}+\frac{\partial^2 u_y}{\partial x\partial y}\right)+\mu\left(1-\ell_2^2\nabla^2\right)\left(\frac{\partial^2 u_x}{\partial y^2}-\frac{\partial^2 u_y}{\partial x\partial y}\right)=0\ , \tag{22}$$

$$\left(\lambda+2\mu\right)\left(1-\ell_1^2\nabla^2\right)\left(\frac{\partial^2 u_x}{\partial x\partial y}+\frac{\partial^2 u_y}{\partial y^2}\right)+\mu\left(1-\ell_2^2\nabla^2\right)\left(\frac{\partial^2 u_y}{\partial x^2}-\frac{\partial^2 u_x}{\partial x\partial y}\right)=0\,. \tag{23}$$

Finally, we note that in the case of a flat boundary defined by the unit normal vector $\mathbf{n}=\left(0,1\right)$, the force and dipole force tractions defined in Eqs. (5) and (6) assume the following form

$$P_x^{(n)}=\tau_{yx}-\frac{\partial m_{xyx}}{\partial x}-\frac{\partial m_{yyx}}{\partial y}-\frac{\partial m_{yxx}}{\partial x}\,,\quad P_y^{(n)}=\tau_{yy}-\frac{\partial m_{xyy}}{\partial x}-\frac{\partial m_{yyy}}{\partial y}-\frac{\partial m_{yxy}}{\partial x}\,, \tag{24}$$

$$R_x^{(n)}=m_{yyx}\,,\quad R_y^{(n)}=m_{yyy}\,. \tag{25}$$

The connection of the tractions $\left(P_q^{(n)},R_q^{(n)}\right)$ with the true tractions $\left(t_q^{(n)},T_{pq}^{(n)}\right)$ defined in Eqs (8) and (9) is given as follows

$$P_x^{(n)}=t_x^{(n)}-\partial_x T_{xx}^{(n)}\,,\quad P_y^{(n)}=t_y^{(n)}-\partial_x T_{xy}^{(n)}\,,\quad R_x^{(n)}=T_{yx}^{(n)}\,,\quad R_y^{(n)}=T_{yy}^{(n)}\,. \tag{26}$$

Note that the tractions $T_{xx}^{(n)}$ and $T_{xy}^{(n)}$ are defined implicitly on the boundary through their surface derivatives, as Eq. (26) suggests. Examples of these dipolar tractions are given in Section 4 (Fig. 1).

4. Half-plane Green's functions in strain-gradient elasticity

In this Section, we consider the plane-strain problem of a half-plane under the action of various types of concentrated surface tractions (line loads) within the context of the complete Toupin-Mindlin gradient elasticity theory. Let D be the open half-plane ($-\infty<x<\infty$, $y>0$) with the straight line boundary L ($y=0$). Depending on the type of the applied surface tractions, *six* fundamental cases can be distinguished accompanied by the following boundary conditions in terms of the *true* force and dipole-force tractions given implicitly in Eq. (26), or equivalently the *auxiliary* force and dipole-force tractions given in Eqs. (24)-(25), which at the surface of the half-plane ($-\infty<x<\infty$, $y=0$) assume the following form (Fig. 1)

Case A. *Concentrated normal force*

$$t_y^{(n)}=P\delta\left(x\right),\quad t_x^{(n)}=0\,,\quad T_{yx}^{(n)}=T_{yy}^{(n)}=T_{xy}^{(n)}=T_{xx}^{(n)}=0\,, \tag{27}$$

or equivalently

$$P_y^{(n)} = P\delta(x), \quad P_x^{(n)} = 0, \quad R_x^{(n)} = R_y^{(n)} = 0. \tag{28}$$

Case B. *Concentrated tangential force*

$$t_x^{(n)} = S\delta(x), \quad t_y^{(n)} = 0, \quad T_{yx}^{(n)} = T_{yy}^{(n)} = T_{xy}^{(n)} = T_{xx}^{(n)} = 0, \tag{29}$$

or equivalently

$$P_x^{(n)} = S\delta(x), \quad P_y^{(n)} = 0, \quad R_x^{(n)} = R_y^{(n)} = 0. \tag{30}$$

Case C. *Concentrated dipole force with moment in the x-direction*

$$T_{yx}^{(n)} = M\delta(x), \quad t_x^{(n)} = t_y^{(n)} = 0, \quad T_{yy}^{(n)} = T_{xy}^{(n)} = T_{xx}^{(n)} = 0, \tag{31}$$

or equivalently

$$R_x^{(n)}(x,0) = M\delta(x), \quad P_x^{(n)} = P_y^{(n)} = 0, \quad R_y^{(n)} = 0. \tag{32}$$

Case D. *Concentrated dipole force without moment in the y-direction*

$$T_{yy}^{(n)} = T\delta(x), \quad t_x^{(n)} = t_y^{(n)} = 0, \quad T_{yx}^{(n)} = T_{xy}^{(n)} = T_{xx}^{(n)} = 0, \tag{33}$$

or equivalently

$$R_y^{(n)}(x,0) = T\delta(x), \quad P_x^{(n)} = P_y^{(n)} = 0, \quad R_x^{(n)} = 0. \tag{34}$$

Case E. *Concentrated dipole force with moment in the y-direction*

$$T_{xy}^{(n)} = Q\delta(x), \quad t_x^{(n)} = t_y^{(n)} = 0, \quad T_{yy}^{(n)} = T_{yx}^{(n)} = T_{xx}^{(n)} = 0, \tag{35}$$

or equivalently

$$P_y^{(n)}(x,0) = -Q\delta'(x), \quad P_x^{(n)} = 0, \quad R_x^{(n)} = R_y^{(n)} = 0. \tag{36}$$

Case F. *Concentrated dipole force without moment in the x-direction*

$$T_{xx}^{(n)} = N\delta(x), \quad t_x^{(n)} = t_y^{(n)} = 0, \quad T_{yy}^{(n)} = T_{yx}^{(n)} = T_{xy}^{(n)} = 0, \tag{37}$$

or equivalently

$$P_x^{(n)}(x,0) = -N\delta'(x), \quad P_y^{(n)} = 0, \quad R_x^{(n)} = R_y^{(n)} = 0. \tag{38}$$

In the above equations, $\delta(x)$ is the Dirac delta function, the prime denotes differentiation with respect to the *x*-variable, and (P,S,T,M,N,Q) are the intensities of the concentrated tractions. In particular, (P,S) are expressed in dimensions of [force][length]$^{-1}$, while (M,T,Q,N) are expressed in dimensions of [force].The six representative cases are depicted schematically in Figure 1.

Note that since D is an unbounded region, the above boundary conditions must be supplemented by the regularity conditions at infinity

$$\tau_{pq},\ m_{pqk} \to 0 \quad \text{as} \quad r \equiv \sqrt{x^2 + y^2} \to \infty\ . \tag{39}$$

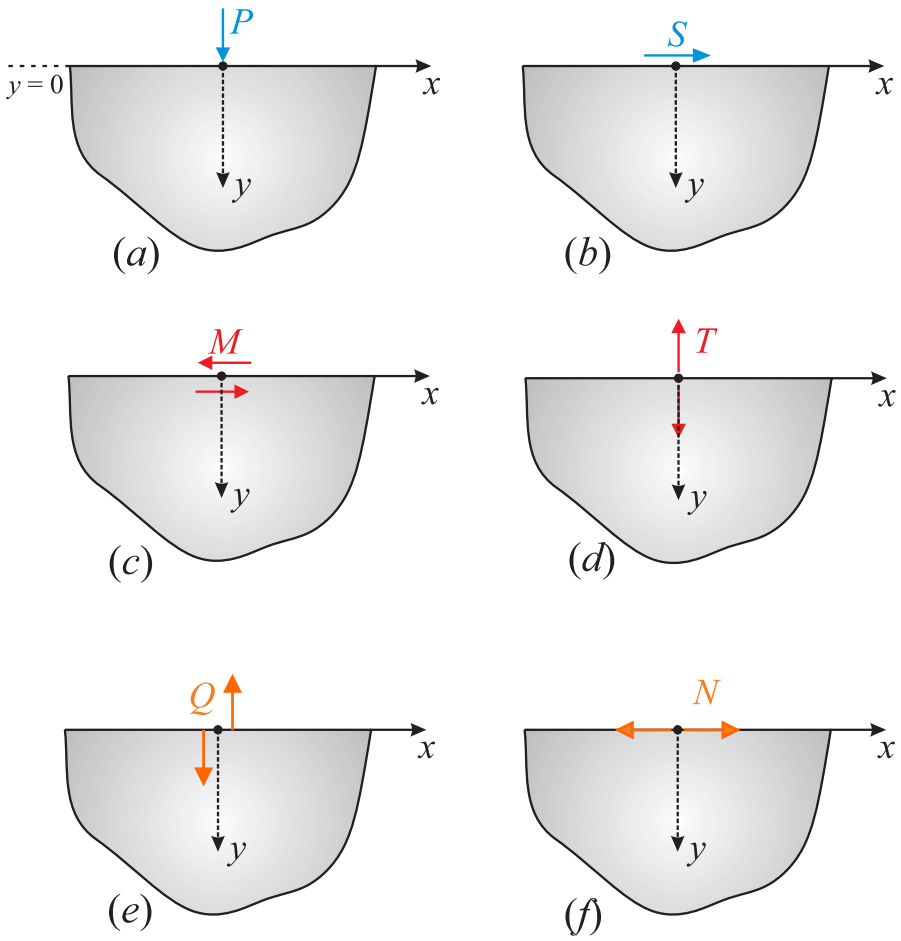

Figure 1: Elastic strain-gradient half-plane loaded at its surface with a concentrated: **(*a*)** normal force **(*b*)** tangential force **(*c*)** dipole force with moment in the x-direction **(*d*)** dipole force without moment in the y-direction, **(*e*)** dipole force with moment in the y-direction **(*f*)** dipole force without moment in the x-direction.

The following point now deserves attention: in plane-strain gradient elasticity we can define *six* types of concentrated surface loads in a half-plane through the use of the true tractions $t_q^{(n)}$ and $T_{pq}^{(n)}$. These tractions are then connected with the *four* auxiliary tractions $P_q^{(n)}$ and $R_q^{(n)}$ through the relations (26). The latter are used for the solution of the pertinent traction boundary value problems (cases (A)-(F)). In particular, cases (A) and (B) are the counterparts of the classical Flamant problem in strain-gradient elasticity. Cases (C) and (D) have no classical counterpart and can be defined only in the context of strain-gradient theory. Finally, cases (E) and (F) can be directly defined through the employment of the true dipolar tractions $T_{xx}^{(n)}$ and $T_{xy}^{(n)}$. In the classical theory, the respective cases are obtained only by the superposition of two opposite normal or tangential forces, respectively, where the distance between them tends to zero (e.g. Timoshenko, 1970). Note that an analogous superposition

scheme *does not* apply in cases (C) and (D). It is perhaps remarkable that a *uniform* distribution of the true dipolar tractions $T_{xx}^{(n)}$ and $T_{xy}^{(n)}$ along the surface of the half-plane ($y=0$) does *not* produce any deformation in the body. Indeed, in this case, according to Eq. (26), the surface derivatives of these quantities and, accordingly, all auxiliary tractions become zero ($P_q^{(n)}=R_q^{(n)}=0$) resulting to a null solution. This situation closely resembles the case of Kirchhoff plates (constrained plate theory) where a uniform distribution of twisting couples at a free edge produces no flexure (Kelvin and Tait, 1895: p. 192, section 647).

The plane-strain traction boundary value problems for the half-plane, corresponding to Cases (A)-(F) are conveniently attacked with the aid of the Fourier transform. The direct Fourier transform and its inverse are defined as follows

$$\hat{f}(\xi)=\int_{-\infty}^{\infty} f(x)\,e^{i\xi x}dx\,,\qquad f(x)=\frac{1}{2\pi}\int_{-\infty}^{\infty}\hat{f}(\xi)\,e^{-i\xi x}d\xi\,, \tag{40}$$

where $i\equiv(-1)^{1/2}$. Transforming the equations of equilibrium (22) and (23) with the aid of $(40)_1$, we obtain a system of differential equations for the transformed displacements $\hat{u}_x(\xi,y)$ and $\hat{u}_y(\xi,y)$ that can be written in compact form as:

$$[K]\begin{bmatrix}\hat{u}_x\\ \hat{u}_y\end{bmatrix}=\begin{bmatrix}0\\ 0\end{bmatrix}, \tag{41}$$

where $[K]$ is the differential operator that reads

$$[K]=\begin{bmatrix}q_{11} & q_{12}\\ q_{21} & q_{22}\end{bmatrix}, \tag{42}$$

with components

$$\begin{aligned}
q_{11}&=\left[\mu d^2-(\lambda+2\mu)\xi^2\right]+\left[(\lambda+2\mu)\ell_1^2\xi^2-\mu\ell_2^2 d^2\right]\left(d^2-\xi^2\right),\\
q_{12}=q_{21}&=-i(\lambda+\mu)\xi d+i\xi d\left[(\lambda+2\mu)\ell_1^2-\mu\ell_2^2\right]\left(d^2-\xi^2\right),
\end{aligned} \tag{43}$$

$$q_{22}=\left[\left(\lambda+2\mu\right)d^{2}-\mu\xi^{2}\right]-\left[\left(\lambda+2\mu\right)\ell_{1}^{2}\,d^{2}-\mu\ell_{2}^{2}\xi^{2}\right]\left(d^{2}-\xi^{2}\right),$$

where $d^{n}\equiv d^{n}\left(\ \right)/dy^{n}$. The system of ODEs in (41) has a non-trivial solution if and only if the determinant of $\left[K\right]$ is equal to zero (Sneddon, 1975). Hence,

$$\det\left[K\right]=\mu\left(\lambda+2\mu\right)\left(d^{2}-\xi^{2}\right)^{2}\left[1-\ell_{1}^{2}\left(d^{2}-\xi^{2}\right)\right]\left[1-\ell_{2}^{2}\left(d^{2}-\xi^{2}\right)\right]=0\ . \tag{44}$$

Equation (44) has the two double roots: $d=\pm\left|\xi\right|$ as in the classical elasticity case, and four single roots: $d=\pm\left(1/\ell_{1}^{2}+\xi^{2}\right)^{1/2}$ and $d=\pm\left(1/\ell_{2}^{2}+\xi^{2}\right)^{1/2}$ which correspond to the presence of the gradient effects. Accordingly, after some rather extensive algebra, a bounded transformed solution of (41) is obtained as $y\to+\infty$

$$\hat{u}_{x}\left(\xi,y\right)=i\left[\left(B_{1}+B_{2}y\right)\mathrm{sgn}\left(\xi\right)-B_{2}\left(3-4\nu\right)\xi^{-1}\right]e^{-|\xi|y}+iB_{3}\,\xi\,\gamma_{1}^{-1}e^{-\gamma_{1}y}+iB_{4}\,\xi^{-1}\,\gamma_{2}e^{-\gamma_{2}y}\ , \tag{45}$$

$$\hat{u}_{y}\left(\xi,y\right)=\left(B_{1}+B_{2}y\right)e^{-|\xi|y}+B_{3}e^{-\gamma_{1}y}+B_{4}e^{-\gamma_{2}y}, \tag{46}$$

where $\gamma_{1}\equiv\gamma_{1}\left(\xi\right)=\left(\ell_{1}^{-2}+\xi^{2}\right)^{1/2}$, $\gamma_{2}\equiv\gamma_{2}\left(\xi\right)=\left(\ell_{2}^{-2}+\xi^{2}\right)^{1/2}$, and $\mathrm{sgn}\left(\ \right)$ is the sign function. Note that for the derivation of Eqs. (45) and (46) use of the relation $\lambda=2\mu\nu\left(1-2\nu\right)^{-1}$ has been made, relating the Lame's constant λ with the Poisson's ratio ν.

The functions $B_{q}\equiv B_{q}\left(\xi\right)$ $(q=1,...,4)$ and accordingly the transformed displacements will be determined through the enforcement of the appropriate boundary conditions for each case of plane-strain problem described above.

In what follows, we focus attention on the evaluation of the *surface* displacements and strains (i.e. for $y=0$), with a view towards obtaining an explicit analytical solution. Notice, however, that determining the field at points 'inside' the half-space ($y>0$) follows along the same general lines of the present analysis but it involves additional numerical work because of the presence of the exponential terms in Eqs. (45) and (46). The present solution is intended to determine the behavior of the displacement and strain fields near to the point of application of the concentrated loads and will allow detecting possible deviations from the predictions of classical theory. In addition, comparison of the present results will be made with the corresponding ones obtained using the *simplified* theory of

gradient elasticity (involving only one gradient parameter - Georgiadis and Anagnostou, 2008) in order to highlight the role of the additional gradient parameters in the *complete* Toupin-Mindlin theory of gradient elasticity.

Finally, it is noted that since the solution procedure to be followed is essentially the same for all the six cases, it will suffice to consider in detail only Case (A) which corresponds to a concentrated normal force acting upon a strain-gradient elastic half-plane.

4.1 Case (A). Concentrated normal force

The first traction boundary value problem under investigation describes the celebrated Flamant problem (see e.g. Timoshenko 1970; Barber, 1992). The elastic half-plane is acted upon by a normal line load P at the origin of the Cartesian rectangular coordinate system (see Fig. 1a).

The solution procedure follows the steps shown in Georgiadis and Anagnostou (2008). In particular, subjecting the boundary conditions (28) to the Fourier transform $(40)_1$ gives rise to a non-homogeneous 4×4 algebraic system from the solution of which the unknown functions $B_q(\xi)$ are subsequently obtained. The expressions for the functions $B_q(\xi)$ are quite lengthy and are not shown here. Exploiting the symmetry of the Flamant problem, the surface displacement field can be expressed by the following inverse Fourier integrals

$$u_x^{(P)}(x,y=0)=-\frac{i}{\pi}\int_0^{\infty}\hat{u}_x^{(P)}(\xi,y=0)\sin(\xi x)\,d\xi\ , \tag{47}$$

$$u_y^{(P)}(x,y=0)=\frac{1}{\pi}\int_0^{\infty}\hat{u}_y^{(P)}(\xi,y=0)\cos(\xi x)\,d\xi\ , \tag{48}$$

where the evenness/oddness of the transformed displacement components:

$$\hat{u}_x^{(P)}(-\xi,y)=-\hat{u}_x^{(P)}(\xi,y),\qquad \hat{u}_y^{(P)}(-\xi,y)=\hat{u}_y^{(P)}(\xi,y), \tag{49}$$

has been taken into account in Eqs (47) and (48).

Next, by using partial-fraction decompositions, the surface displacements can be written in terms of three integrals, in the following form

$$u_x^{(P)}(x,y=0)=I_{class}^{(P)}(x)+I_{grad-1}^{(P)}(x)+I_{grad-2}^{(P)}(x)\ , \tag{50}$$

$$u_y^{(P)}\left(x,y=0\right)=J_{class}^{(P)}\left(x\right)+J_{grad-1}^{(P)}\left(x\right)+J_{grad-2}^{(P)}\left(x\right)\ , \tag{51}$$

with

$$I_{class}^{(P)}\left(x\right)=-\frac{P\left(1-2\nu\right)}{2\pi\mu}\int_0^\infty\frac{1}{\xi}\sin\left(\xi x\right)d\xi=-\frac{P\left(1-2\nu\right)}{4\mu}\mathrm{sgn}\left(x\right), \tag{52}$$

$$I_{grad-1}^{(P)}\left(x\right)=\frac{P\left(1-2\nu\right)}{2\pi\mu}\int_0^\infty\frac{\ell_2^2\,\xi}{1+\ell_2^2\,\xi^2}\sin\left(\xi x\right)d\xi=\frac{P\left(1-2\nu\right)}{4\mu}\mathrm{sgn}\left(x\right)\mathrm{e}^{-\left|x\right|/\ell_2}, \tag{53}$$

$$I_{grad-2}^{(P)}\left(x\right)=\frac{1}{\pi}\int_0^\infty\left[-i\,\hat{u}_x^{(P)}\left(\xi,0\right)+\frac{P\left(1-2\nu\right)}{2\mu\xi\left(1+\ell_2^2\,\xi^2\right)}\right]\sin\left(\xi x\right)d\xi\,, \tag{54}$$

and

$$J_{class}^{(P)}\left(x\right)=\frac{P\left(1-\nu\right)}{\pi\mu}\textbf{F.P.}\int_0^\infty\frac{1}{\xi}\cos\left(\xi x\right)d\xi=-\frac{P\left(1-\nu\right)}{\pi\mu}\ln\left|x\right|, \tag{55}$$

$$J_{grad-1}^{(P)}\left(x\right)=-\frac{P\left(1-\nu\right)}{\pi\mu}\int_0^\infty\frac{\ell_2}{\left(1+\ell_2^2\,\xi^2\right)^{1/2}}\cos\left(\xi x\right)d\xi=-\frac{P\left(1-\nu\right)}{\pi\mu}K_0\left[\left|x\right|/\ell_2\right], \tag{56}$$

$$J_{grad-2}^{(P)}\left(x\right)=\frac{1}{\pi}\int_0^\infty\left[\hat{u}_y^{(P)}\left(\xi,0\right)-\frac{P\left(1-\nu\right)}{\mu}\frac{\left(1+\ell_2^2\,\xi^2\right)^{1/2}-\ell_2\xi}{\xi\left(1+\ell_2^2\,\xi^2\right)^{1/2}}\right]\cos\left(\xi x\right)d\xi\,, \tag{57}$$

where $K_0\left[\ \right]$ is the modified Bessel function of the second kind and the symbol **F.P.** denotes finite-part integration.

In view of the above, the final expressions for the displacement components in the Toupin-Mindlin theory of strain-gradient elasticity read

$$u_x^{(P)}\left(x,y=0\right)=\frac{P\left(1-2\nu\right)}{4\mu}\mathrm{sgn}\left(x\right)\left(e^{-\left|x\right|/\ell_2}-1\right)+I_{grad-2}^{(P)}\left(x\right), \tag{58}$$

$$u_y^{(P)}\left(x,y=0\right)=-\frac{P\left(1-\nu\right)}{\pi\mu}\left(\ln\left|x\right|+K_0\left[\left|x\right|/\ell_2\right]\right)+J_{grad-2}^{(P)}\left(x\right). \tag{59}$$

In the limit case of classical linear elasticity, the second and third terms in the RHS of each one of equations (58)-(59) vanish and the surface displacements are then provided by the following relations

$$u_{x\ (class.)}^{(P)}\left(x,y=0\right)=-\frac{P\left(1-2\nu\right)}{4\mu}\mathrm{sgn}\left(x\right), \tag{60}$$

$$u_{y\ (class.)}^{(P)}\left(x,y=0\right)=-\frac{P\left(1-\nu\right)}{\pi\mu}\ln\left|x\right|, \tag{61}$$

i.e. a solution which is discontinuous and unbounded at the point of application of the concentrated force (Barber, 1992).

Regarding the behavior of the gradient solution near to the point of application of the concentrated load, we note first that functions defined by the integrals in Eqs (54) and (57) are bounded and continuous as $\left|x\right|\to 0$

$$\lim_{|x|\to 0} I_{grad-2}^{(P)}\left(x\right)=O\left(1\right) \quad \text{and} \quad \lim_{|x|\to 0} J_{grad-2}^{(P)}\left(x\right)=O\left(1\right). \tag{62}$$

Moreover, taking into account that: $\lim_{|x|\to 0} K_0\left(x\right)=-O\left(\ln\left|x\right|\right)$, it can be readily inferred from (59) that the logarithmic singularity of $u_y^{(P)}\left(x,0\right)$ predicted by the classical theory is eliminated in the context of the complete Toupin-Mindlin theory. In addition, in view of Eqs (52), (53), and (62), the discontinuity of $u_x^{(P)}\left(x,0\right)$ attained in the classical elasticity disappears. However, the normal displacement at infinity remains logarithmically unbounded as in the classical theory, since away from the origin the strain-gradient effects decay and the classical elasticity solution dominates. Such a pathological behavior is known in 2D elastostatic problems involving concentrated loads in the context of classical elasticity and couple-stress elasticity (see e.g. Turteltaub and Sternberg 1968; Bigoni and Gourgiotis 2016).

Finally, using asymptotic analysis it can be shown that in the Toupin-Mindlin theory of gradient elasticity the strain components ε_{pq} are *bounded* at the point of application of the force, whereas the strain gradients κ_{rpq} exhibit a *logarithmic* singularity as $r\to 0$. The observation that the both displacements and strains are bounded in the Flamant problem was first made by Lardner (1970). The boundness of the strain field implies, accordingly, that the monopolar stresses τ_{pq} are also bounded at the origin, a result which is in marked contrast with the predictions of the classical theory where simple equilibrium considerations dictate that these stresses exhibit a r^{-1} singularity. On the other hand, as it

will be shown in more detail in section 5, the dipolar stresses m_{rpq} become logarithmically unbounded at the point of application of the force.

In view of the above results, it can be readily inferred that the strain-energy density W defined in (1) behaves at most as: $W \approx O\left(\partial_k \varepsilon_{pq}\right)^2 \approx O\left(\ln r\right)^2$, which, in turn, implies that the (total) strain energy in any (non-zero) area surrounding the concentrated load is *finite*. The latter observation shows that the Kirchhoff-type theorem established for strain-gradient elasticity (Grentzelou and Georgiadis, 2005) guarantees uniqueness of solution (within a rigid body field) in the present problem. Note that analogous results hold for the 3D problems of Boussinesq and Cerruti (Georgiadis et al., 2014; Anagnostou et al., 2013) in strain-gradient elasticity.

4.2 Case (*B*)*. Concentrated tangential force*

In this case, the elastic half-plane is acted upon by a tangential line load S at the origin of the Cartesian rectangular coordinate system (see Fig. 1b). Following an analogous analysis as the one outlined in section 4.1, the components of the displacement vector assume the following form

$$u_x^{(S)}\left(x, y=0\right) = \frac{1}{\pi}\int_0^\infty \hat{u}_x^{(S)}\left(\xi, y=0\right)\cos\left(\xi x\right)d\xi \ , \tag{63}$$

$$u_y^{(S)}\left(x, y=0\right) = -\frac{i}{\pi}\int_0^\infty \hat{u}_y^{(S)}\left(\xi, y=0\right)\sin\left(\xi x\right)d\xi \ , \tag{64}$$

where the evenness/oddness of the transformed displacement components has been taken into account in the above equations. The surface displacements can then be written again in terms of three integrals as

$$u_x^{(S)}\left(x, y=0\right) = I_{class}^{(S)}\left(x\right) + I_{grad-1}^{(S)}\left(x\right) + I_{grad-2}^{(S)}\left(x\right) \ , \tag{65}$$

$$u_y^{(S)}\left(x, y=0\right) = J_{class}^{(S)}\left(x\right) + J_{grad-1}^{(S)}\left(x\right) + J_{grad-2}^{(S)}\left(x\right) \ , \tag{66}$$

where

$$I_{class}^{(S)}\left(x\right) = \frac{S\left(1-\nu\right)}{\pi\mu}\mathbf{F.P.}\int_0^\infty \frac{1}{\xi}\cos\left(\xi x\right)d\xi = -\frac{S\left(1-\nu\right)}{\pi\mu}\ln\left|x\right| \ , \tag{67}$$

$$I_{grad-1}^{(S)}(x)=-\frac{S(1-\nu)}{\pi\mu}\int_0^{\infty}\frac{\ell_2}{\left(1+\ell_2^2\xi^2\right)^{1/2}}\cos(\xi x)\,d\xi=-\frac{S(1-\nu)}{\pi\mu}K_0\left[|x|/\ell_2\right], \tag{68}$$

$$I_{grad-2}^{(S)}(x)=\frac{1}{\pi}\int_0^{\infty}\left[\hat{u}_x^{(S)}(\xi,0)-\frac{S(1-\nu)}{\mu}\frac{\left(1+\ell_2^2\,\xi^2\right)^{1/2}-\ell_2\xi}{\xi\left(1+\ell_2^2\,\xi^2\right)^{1/2}}\right]\cos(\xi x)\,d\xi\,, \tag{69}$$

and

$$J_{class}^{(S)}(x)=\frac{S(1-2\nu)}{2\pi\mu}\int_0^{\infty}\frac{1}{\xi}\sin(\xi x)\,d\xi=\frac{S(1-2\nu)}{4\mu}\mathrm{sgn}(x), \tag{70}$$

$$J_{grad-1}^{(S)}(x)=-\frac{S(1-2\nu)}{2\pi\mu}\int_0^{\infty}\frac{\ell_2^2\,\xi}{1+\ell_2^2\,\xi^2}\sin(\xi x)\,d\xi=-\frac{S(1-2\nu)}{4\mu}\mathrm{sgn}(x)\mathrm{e}^{-|x|/\ell_2}\,, \tag{71}$$

$$J_{grad-2}^{(S)}(x)=-\frac{1}{\pi}\int_0^{\infty}\left[i\,\hat{u}_y^{(S)}(\xi,0)+\frac{S(1-2\nu)}{2\mu}\frac{1}{\xi\left(1+\ell_2^2\;\xi^2\right)}\right]\sin(\xi x)\,d\xi\,. \tag{72}$$

In view of the above, the final expressions for the displacement components in the Toupin-Mindlin theory of strain-gradient elasticity read

$$u_x^{(S)}(x,y=0)=-\frac{S(1-\nu)}{\pi\mu}\left(\ln|x|+K_0\left[|x|/\ell_2\right]\right)+I_{grad-2}^{(S)}(x), \tag{73}$$

$$u_y^{(S)}(x,y=0)=\frac{S(1-2\nu)}{4\mu}\mathrm{sgn}(x)\left(1-e^{-|x|/\ell_2}\right)+J_{grad-2}^{(S)}(x)\,. \tag{74}$$

In the limit case of classical linear elasticity, the second and third terms in the RHS of each one of equations (73)-(74) vanish and the surface displacements are then provided by the following relations

$$u_{x\ (class.)}^{(S)}(x,y=0)=-\frac{S(1-\nu)}{\pi\mu}\ln|x|\,, \tag{75}$$

$$u_{y\ (class.)}^{(S)}(x,y=0)=\frac{S(1-2\nu)}{4\mu}\mathrm{sgn}(x)\,. \tag{76}$$

Regarding the behavior of the solution near to the point of application of the concentrated load, we note first that functions defined by the integrals in Eqs (69) and (72) are bounded and continuous as $|x| \to 0$. Accordingly, the surface tangential displacement $u_x^{(S)}(x,0)$ is bounded in the context of the complete Toupin-Mindlin theory, whereas the discontinuity of $u_y^{(S)}(x,0)$ attained in the classical elasticity is eliminated.

Finally, we note that as in the classical theory of elasticity, the reciprocal relation: $\left|P \cdot u_y^{(S)}\right| = \left|S \cdot u_x^{(P)}\right|$ holds true in view of the Betti-Rayleigh reciprocal theorem established by Georgiadis and Grentzelou (2006) for strain-gradient elasticity (see also Georgiadis and Anagnostou, 2008; Agiasofitou and Lazar, 2009).

4.3 Case (C). Concentrated force dipole with moment in the x-direction

In this case, the elastic half-plane is loaded by a concentrated force dipole M (Fig. 1c). The boundary conditions at the surface of the half-plane ($y=0$) are given in (32), whereas the components of the displacement vector can be written in the following form

$$u_x^{(M)}(x, y=0) = \frac{1}{\pi}\int_0^\infty \hat{u}_y^{(M)}(\xi, y=0)\cos(\xi x)\, d\xi\,, \tag{77}$$

$$u_y^{(M)}(x, y=0) = -\frac{i}{\pi}\int_0^\infty \hat{u}_x^{(M)}(\xi, y=0)\sin(\xi x)\, d\xi\,, \tag{78}$$

taking into account the evenness/oddness of the transformed displacements. The expressions for the transformed displacements in (77) and (78) are lengthy and are not shown here. The above Fourier integrals are convergent as $x \to 0$ and thus can be directly evaluated taking into account their oscillatory character.

It is remarked that in the simplified (3-parameter) gradient elasticity theory the transformed surface displacements assume the simple form:

$$\hat{u}_x^{(M)}(\xi, y=0) = \frac{M(1-\nu)\left(3+2\ell^2\xi(\gamma+2\xi)-\nu\left(2+4\ell^2\xi(\gamma+\xi)\right)\right)}{2\mu N(\xi)}\,, \tag{79}$$

$$\hat{u}_y^{(M)}(\xi, y=0) = \frac{iM(1-\nu)\left(1+\ell^2\xi(\gamma+2\xi)-\nu\left(1+2\ell^2\xi(\gamma+\xi)\right)\right)}{\mu N(\xi)}\,. \tag{80}$$

where $\gamma \equiv \gamma(\xi) = \left(\ell^{-2} + \xi^2\right)^{1/2}$ and

$$N(\xi) = -1 + \nu\left(1 + 2\ell^2\xi^2\right)\left(1 + 2\ell^2\xi(\gamma + \xi)\right) - 2\ell^2\xi\left(\gamma + \xi\left(3 + \ell^2\xi(2\gamma + 3\xi)\right)\right). \tag{81}$$

Note that case C has no counterpart in the classical elasticity theory.

4.4 Case (*D*)*. Concentrated force dipole without moment in the y-direction*

In this case, the elastic half-plane is loaded by a concentrated dipole force without moment T (Fig. 1d). The boundary conditions at the surface of the half-plane ($y = 0$) are given in (34) and the components of the displacement vector can be written as

$$u_x^{(T)}(x, y = 0) = -\frac{i}{\pi}\int_0^\infty \hat{u}_x^{(T)}(\xi, y = 0)\sin(\xi x)\, d\xi\,, \tag{82}$$

$$u_y^{(T)}(x, y = 0) = \frac{1}{\pi}\int_0^\infty \hat{u}_y^{(T)}(\xi, y = 0)\cos(\xi x)\, d\xi\,. \tag{83}$$

The expressions for the transformed surface displacements in (82) and (83) are lengthy and are not presented here. In the case of the simplified (3-parameter) gradient elasticity the transformed surface displacements assume the simple form

$$\hat{u}_x^{(T)}(\xi, y = 0) = -\frac{iT\left(\ell^2\gamma\xi + 2\nu\left(-1 + \nu - \ell^2\gamma(3 - 2\nu)\xi - 2\ell^2(1 - \nu)\xi^2\right)\right)}{2\mu N(\xi)}\,, \tag{84}$$

$$\hat{u}_y^{(T)}(\xi, y = 0) = \frac{T(1 - \nu)\left(1 + 2\ell^2\xi(\gamma + 2\xi) - \nu\left(2 + 4\ell^2\xi(\gamma + \xi)\right)\right)}{2\mu N(\xi)}\,. \tag{85}$$

Note that case D has no counterpart in the classical elasticity theory. A structural mechanics analogue of such similar self-equilibrating dipolar forces without moment can be found in the bending analysis of a beam with a *T*-type cross-section (Vardoulakis and Giannakopoulos, 2006).

Finally, we remark that according to the reciprocal theorem in strain-gradient elasticity (Georgiadis and Grentzelou, 2006), the following relation holds true: $\left|M \cdot \partial_y u_x^{(T)}\right| = \left|T \cdot \partial_y u_y^{(M)}\right|$.

4.5 Case (*E*). *Concentrated force dipole with moment in the y-direction*

In this case, the elastic half-plane is loaded by a concentrated dipole force with moment in the *y*-direction (Fig. 1e). The boundary conditions are given in Eqs (36). As it can be readily seen from Eq. $(26)_2$, the non-zero traction $P_y^{(n)}$ is implicitly connected with the surface derivative of the dipole traction $T_{xy}^{(n)}$. Therefore, in the context of strain-gradient elasticity such a concentrated couple can be directly incorporated through the enforcement of the boundary condition: $T_{xy}^{(n)} = Q\delta(x)$. On the other hand, in the context of classical elasticity, such a concentrated couple can be generated only indirectly by the superposition of two normal to the boundary concentrated forces with opposite directions placed at an infinitesimal distance to each other. The problem of a concentrated couple in classical elasticity was examined (among others) by Timoshenko (1970).

The components of the displacement vector can be written as

$$u_x^{(Q)}(x, y=0) = -\frac{i}{\pi}\int_0^\infty \hat{u}_x^{(Q)}(\xi, y=0)\sin(\xi x)\, d\xi, \tag{86}$$

$$u_y^{(Q)}(x, y=0) = \frac{1}{\pi}\int_0^\infty \hat{u}_y^{(Q)}(\xi, y=0)\cos(\xi x)\, d\xi, \tag{87}$$

4.6 Case (*F*)*. Concentrated force dipole without moment in the x-direction*

In this case, the elastic half-plane is loaded by a concentrated force dipole without moment in the *x*-direction (Fig. 1f). The boundary conditions are given in Eqs (38). Similarly to case (E), the non-zero traction $P_x^{(n)}$ is implicitly connected with the surface derivative of the dipole traction $T_{xx}^{(n)}$ through Eq. $(26)_1$. Therefore, in the context of strain-gradient elasticity such a concentrated dipole can be directly incorporated through the enforcement of the boundary condition: $T_{xx}^{(n)} = N\delta(x)$. On the other hand, in the context of classical elasticity, a concentrated dipole without moment can be generated only indirectly by the superposition of two tangential to the boundary concentrated forces with opposite directions placed at an infinitesimal distance to each other.

5. On the role of edge forces in strain-gradient elasticity

In this Section, the role of edge forces (Eq. (7)) arising in strain-gradient elasticity is elucidated using simple equilibrium considerations in the case of a half-plane loaded by a concentrated normal force P (case A). For simplicity, the *simplified* gradient elasticity theory is employed here, nonetheless the results obtained apply also in the complete Toupin-Mindlin theory of strain-gradient elasticity. It is recalled that for the *simplified* gradient elasticity case: $\ell_1 = \ell_2 = \ell$.

The role of edge forces in strain-gradient elasticity was first investigated by Green and Naghdi (1968), who illustrated how these forces contribute in the equilibrium of a finite cylinder under pure torsion. Recently, the role of these edge forces was highlighted in crack problems by Gourgiotis et al. (2010), and Sciarra and Vidoli (2012), and by Charalambopoulos and Polyzos (2015) who studied a simple 2D problem of an elastic rectangle subjected to different types of boundary conditions.

We consider a semi-circular sector of radius r_0 and attach a polar coordinate system (r,θ) at the point of application of the concentrated force (Fig. 2). Along the circular arc $\overset{\frown}{AB}$ the outward unit normal vector is $\mathbf{n}=\mathbf{e}_r$ whereas along the traction-free plane surface becomes $\mathbf{n}=-\mathbf{e}_y$. As it can be seen from Figure 2, two straight edges are formed lying parallel to the z-axis with unit tangent vector $\mathbf{s}=(0,0,1)$ and passing through the corner points $A(r_0,\theta=0)$ and $B(r_0,\theta=\pi)$, respectively. Note that $\mathbf{n}$ becomes discontinuous at A and B. In fact, in view of (7), the following geometric relations hold employing the *polar* coordinate system:

$$\text{Point A:}\quad \begin{cases}\mathbf{n}^{+}=(0,-1,0)\\ \mathbf{k}^{+}=\mathbf{s}\times\mathbf{n}^{+}=(1,0,0)\end{cases}\quad\text{and}\quad \begin{cases}\mathbf{n}^{-}=(1,0,0)\\ \mathbf{k}^{-}=\mathbf{s}\times\mathbf{n}^{-}=(0,1,0)\end{cases}, \tag{88}$$

$$\text{Point B:}\quad \begin{cases}\mathbf{n}^{+}=(1,0,0)\\ \mathbf{k}^{+}=\mathbf{s}\times\mathbf{n}^{+}=(0,1,0)\end{cases}\quad\text{and}\quad \begin{cases}\mathbf{n}^{-}=(0,1,0)\\ \mathbf{k}^{-}=\mathbf{s}\times\mathbf{n}^{-}=(-1,0,0)\end{cases}. \tag{89}$$

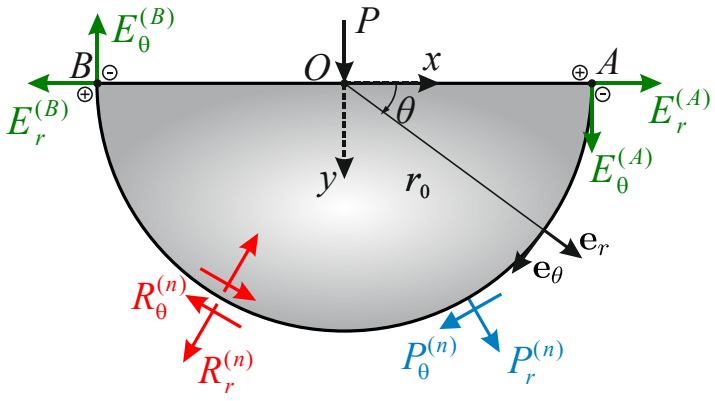

Figure 2. Equilibrium of a semi-circular sector in the Flamant problem in strain-gradient elasticity.

The discontinuity in the outward unit normal vector gives rise to two edge forces E_q (line loads constant along the z-direction) which are exerted upon the two edges (Fig. 2). According to Eq. (7), the polar components of these forces assume the following form:

$$E_r^{(A)} = -m_{r\theta r}\left(r_0,0\right) - m_{\theta rr}\left(r_0,0\right), \qquad E_\theta^{(A)} = -m_{r\theta\theta}\left(r_0,0\right) - m_{\theta r\theta}\left(r_0,0\right), \tag{90}$$

$$E_r^{(B)} = m_{\theta rr}\left(r_0,\pi\right) + m_{r\theta r}\left(r_0,\pi\right), \qquad E_\theta^{(B)} = m_{r\theta\theta}\left(r_0,\pi\right) + m_{\theta r\theta}\left(r_0,\pi\right), \tag{91}$$

Moreover, the expressions for the force tractions $\left(P_r^{(n)}, P_\theta^{(n)}\right)$ and dipolar-force tractions $\left(R_r^{(n)}, R_\theta^{(n)}\right)$ that are distributed along the arc $\widehat{AB}$ become (Gourgiotis et al., 2010)

$$P_r^{(n)} = \tau_{rr} - \frac{\partial m_{rrr}}{\partial r} - \frac{1}{r}\frac{\partial m_{\theta rr}}{\partial \theta} - \frac{1}{r}\frac{\partial m_{r\theta r}}{\partial \theta} - \frac{1}{r}m_{rrr} + \frac{2}{r}m_{\theta\theta r} + \frac{1}{r}m_{r\theta\theta}, \tag{92}$$

$$P_\theta^{(n)} = \tau_{r\theta} - \frac{\partial m_{rr\theta}}{\partial r} - \frac{1}{r}\frac{\partial m_{r\theta\theta}}{\partial \theta} - \frac{1}{r}\frac{\partial m_{\theta r\theta}}{\partial \theta} - \frac{1}{r}m_{\theta rr} - \frac{2}{r}m_{rr\theta} + \frac{1}{r}m_{\theta\theta\theta}, \tag{93}$$

$$R_r^{(n)} = m_{rrr}, \quad R_\theta^{(n)} = m_{rr\theta}. \tag{94}$$

where $\mathbf{n} = \mathbf{e}_r$.

As we shall now show, the role of the edge forces in (90) and (91) is to *balance* the resultant force and moment of the force and dipolar-force tractions acting on the semi-circular arc $\widehat{AB}$. To this purpose, it is expedient to derive the dominant asymptotic stress fields near the point of application of the concentrated force. As it was pointed out in Section 4.1, the monopolar stresses are bounded whereas the dipolar stresses exhibit a logarithmic singularity as $r \to 0$. Hence, the dominant asymptotic behavior of the tractions in (92)-(94) is due to the logarithmically singular dipolar stress field. The latter is found by using the Abel-Tauber theorem and employing results from the theory of generalized functions (Roos, 1969). In particular, with the aid of the elementary expansions (see also Muki and Sternberg, 1965), we obtain within the framework of the simplified strain-gradient elasticity:

$$\gamma_1\left(\xi\right) = \gamma_2\left(\xi\right) = \gamma\left(\xi\right) = \ell^{-1}\left[\left|\xi\right|\ell + \left(2\left|\xi\right|\ell\right)^{-1} + \left(2\left|\xi\right|\ell\right)^{-3}\right] + O\left(\left|\xi\right|^{-5}\right), \tag{95}$$

$$e^{-y\gamma_1} = e^{-y|\xi|}\left[1 - y\left(2\left|\xi\right|\ell^2\right)^{-1} + y^2\left(8\xi^2\ell^4\right)^{-1} + O\left(\left|\xi\right|^{-3}\right)\right], \tag{96}$$

valid for $y \geq 0$ and $\xi \to \infty$, and retaining only the dominant asymptotic terms, the components of the transformed dipolar stress tensor assume can be written as

$$\hat{m}_{xxx} = \frac{iP\left(4-4\nu-y^2\xi^2-2(1-2\nu)\,y|\xi|\right)}{2(5-4\nu)\xi}\, e^{-y|\xi|}\,, \tag{97}$$

$$\hat{m}_{xyy} = \frac{iP\left(6-4\nu+y^2\xi^2+2(3-2\nu)\,y|\xi|\right)}{2(5-4\nu)\xi} e^{-y|\xi|}\,, \tag{98}$$

$$\hat{m}_{yyx} = \frac{iP|\xi|\left(2-4\nu+y|\xi|\right)}{2(5-4\nu)\xi} e^{-y|\xi|}, \tag{99}$$

$$\hat{m}_{xxy} = -\frac{P\left(4-4\nu+y^2\xi^2+4(1-\nu)\,y|\xi|\right)}{2(5-4\nu)|\xi|} e^{-y|\xi|}, \tag{100}$$

$$\hat{m}_{yyy} = \frac{P\,y\left(4-4\nu+y|\xi|\right)}{2(5-4\nu)} e^{-y|\xi|}, \tag{101}$$

$$\hat{m}_{yxx} = \frac{P\left(6-8\nu-y^2\xi^2+4\nu y|\xi|\right)}{2(5-4\nu)|\xi|} e^{-y|\xi|}. \tag{102}$$

Utilizing the inverse Fourier transform $(40)_2$, we can analytically derive the asymptotic behavior of the dipolar stress field as $r \to 0$. The dipolar stress components in polar coordinates finally read

$$m_{rrr}(r,\theta) = \frac{P}{4\pi(5-4\nu)}\Big[4\ln r\,\cos^2\theta\sin\theta+(\pi-2\theta)(5-4\nu-\cos 2\theta)\cos\theta + \left(3+2\beta-(7-2\beta-8\nu)\cos 2\theta\right)\sin\theta\Big], \tag{103}$$

$$m_{rr\theta}(r,\theta) = \frac{P}{4\pi(5-4\nu)}\Big[2\ln r\left(3-4\nu+\cos 2\theta\right)\cos\theta+2(\pi-2\theta)\cos^2\theta\sin\theta + 2\left(4(1-\nu)\beta+(7-2\beta-8\nu)\sin^2\theta\right)\cos\theta\Big], \tag{104}$$

$$m_{\theta rr}(r,\theta) = \frac{P}{4\pi(5-4\nu)}\Big[2\ln r\left(-7+8\nu+\cos 2\theta\right)\cos\theta-(\pi-2\theta)(5-4\nu-\cos 2\theta)\sin\theta + \left((7-8\nu)(1-2\beta)-(7-8\nu-2\beta)\cos 2\theta\right)\cos\theta\Big], \tag{105}$$

$$m_{r\theta\theta}(r,\theta) = \frac{P}{4\pi(5-4\nu)}\Big[2\ln r\left(-7+8\nu-\cos 2\theta\right)\sin\theta+(\pi-2\theta)(5-4\nu+\cos 2\theta)\cos\theta + \left(5-2\beta(7-8\nu)+(7-2\beta-8\nu)\cos 2\theta\right)\sin\theta\Big], \tag{106}$$

$$m_{\theta\theta\theta}(r,\theta)=\frac{P}{4\pi(5-4\nu)}\Big[4\ln r\sin^2\theta\cos\theta-(\pi-2\theta)(5-4\nu+\cos 2\theta)\sin\theta \\ -2(7-2\beta-8\nu)\sin^2\theta\cos\theta\Big], \tag{107}$$

$$m_{\theta\theta r}(r,\theta)=\frac{P}{4\pi(5-4\nu)}\Big[2\ln r(3-4\nu-\cos 2\theta)\sin\theta-2(\pi-2\theta)\sin^2\theta\cos\theta \\ -(3-(6-8\nu)\beta-(7-8\nu-2\beta)\cos 2\theta)\sin\theta\Big], \tag{108}$$

where β ($\beta=0.577$) is the Euler-Mascheroni constant. It is remarked that the above asymptotic field satisfies the dominant part of the equations of equilibrium (4).

Substituting (103)-(108) into (90)-(91), the edge forces at points A and B finally become

$$E_r^{(A)}=\frac{P(1-2\nu)(\ln r+\beta)}{\pi(5-4\nu)},\quad E_\theta^{(A)}=-\frac{P(3-2\nu)}{2(5-4\nu)},\quad E_r^{(B)}=E_r^{(A)},\quad E_\theta^{(B)}=-E_\theta^{(A)}. \tag{109}$$

On the other hand, the resultant force and couple due to the distribution of tractions along the semi-circular arc $\widehat{AB}$ of radius r_0 are

$$\Sigma F_x^{\widehat{(AB)}}=r_0\int_0^\pi\left(P_r^{(n)}\cos\theta-P_\theta^{(n)}\sin\theta\right)d\theta=0, \tag{110}$$

$$\Sigma F_y^{\widehat{(AB)}}=r_0\int_0^\pi\left(P_r^{(n)}\sin\theta+P_\theta^{(n)}\cos\theta\right)d\theta=-\frac{2P(1-\nu)}{5-4\nu}, \tag{111}$$

$$\Sigma M^{\widehat{(AB)}}=r_0\int_0^\pi\left(Q_z^{(n)}+r_0P_\theta^{(n)}\right)d\theta=r_0\int_0^\pi\left(2R_\theta^{(n)}+r_0P_\theta^{(n)}\right)d\theta=0, \tag{112}$$

where $Q_k^{(n)}=2e_{pqk}n_pR_q^{(n)}$ is the tangential component of the moment vector (Mindlin and Eshel, 1967). For the plane strain case considered here the only non-vanishing component of the moment vector is $Q_z^{(n)}$, which on the semi-circular arc $\widehat{AB}$ ($\mathbf{n}=\mathbf{e}_r$) assumes, according to its definition, the form: $Q_z^{(n)}=2R_\theta^{(n)}$. Note further that, in (112) only the dipolar force traction $R_\theta^{(n)}$ contributes in the equilibrium of moments, since $R_r^{(n)}$ is a self-equilibrated traction (see Fig. 2).

The *total* resultant forces in the horizontal and vertical direction and the *total* resultant moment with respect to the origin are written then as

$$\Sigma F_x = \Sigma F_x^{\widehat{(AB)}} + E_r^{(A)} - E_r^{(B)} = 0\,, \tag{113}$$

$$\Sigma F_y = P + \Sigma F_y^{\widehat{(AB)}} + E_\theta^{(A)} - E_\theta^{(B)} = 0\,, \tag{114}$$

$$\Sigma M = \Sigma M^{\widehat{(AB)}} + r_0\left(E_\theta^{(A)} + E_\theta^{(B)}\right) = 0\,, \tag{115}$$

showing that equilibrium is satisfied in a strain-gradient continua only when the edge forces at the corners of the domain are taken into account. These forces are determined *a posteriori* from the solution of the boundary value problem.

6. Results and Discussion

Before we proceed, it is expedient to normalize the components of the displacement and the strain fields for the force and force-dipole problems, respectively, as

$$\begin{aligned} &\overline{u}_i^{(\alpha)} = \mu\, k^{-1}\, u_i^{(\alpha)}\,, \qquad \overline{\varepsilon}_{ij}^{(\alpha)} = \mu \ell_2 k^{-1}\, \varepsilon_{ij}^{(\alpha)}\,, \qquad k = \{P, S\} \\ &\overline{u}_i^{(\beta)} = \mu \ell_2 k^{-1}\, u_i^{(\beta)}\,, \quad \overline{\varepsilon}_{ij}^{(\beta)} = \mu \ell_2^2 k^{-1}\, \varepsilon_{ij}^{(\beta)}\,, \qquad k = \{M, T, Q, N\} \end{aligned} \tag{116}$$

with $(i, j) = (x, y)$. Accordingly, we define the normalized distance from the point loads as: $\overline{x} = x/\ell_2$.

To facilitate numerical computations, we introduce three dimensionless parameters which characterized effectively a strain-gradient material under plane-strain conditions

$$d_0 = \frac{2c_3}{c_2}, \quad d_1 = \frac{2(1-2\nu)}{(1-\nu)}\frac{c_1}{c_2} = \frac{\ell_1^2}{\ell_2^2}, \quad d_2 = \frac{(1-2\nu)}{\nu}\frac{c_4}{c_2}\ . \tag{117}$$

Note that the parameter d_1 is equal to the squared ratio of the characteristic lengths in gradient elasticity. Moreover, the special case $d_0 = d_1 = d_2 = 1$ corresponds to the simplified gradient elasticity. The ranges of the new material parameters in the strain-gradient theory are found by resorting to the condition for positive definiteness (PD) of the strain energy density function. In light of the inequalities in (16), we find that in order for the strain energy density to be (PD) the following inequalities must hold for the above three parameters:

(*i*) $\nu = 0$

$$\begin{cases} 0 < d_0 < \dfrac{15}{8} \\ \dfrac{1}{15}\left(15 + d_0 - \sqrt{(15-2d_0)(15-8d_0)}\right) < d_1 < \dfrac{1}{15}\left(15 + d_0 + \sqrt{(15-2d_0)(15-8d_0)}\right) \end{cases}, \tag{118}$$

(*ii*) $0 < \nu < \dfrac{1}{2}$

$$\begin{cases} 0 < d_0 < \dfrac{15}{8} \\ d_1 > \dfrac{2d_0(1-2\nu)}{5(1-\nu)} \\ r_1 < d_2 < r_2 \end{cases}, \tag{119}$$

where

$$r_{1,2} = \frac{-9d_0(1-2\nu) + 15d_1(1-\nu) \mp \sqrt{6}\sqrt{(1-2\nu)(8d_0-15)\left(2d_0(1-2\nu) - 5d_1(1-\nu)\right)}}{15\nu}. \tag{120}$$

Note that when $\nu = 0$, (PD) conditions do not depend upon the parameter d_2. Similar results were obtained by Eshel and Rosenfeld (1970) using, however, different definitions for the dimensionless gradient parameters.

In what follows, we present selected representative results for the displacement and/or strain fields for the six loading cases described in Section 4. For the shake of brevity, we discuss in detail only case (A) while the other loading cases are briefly commented upon. The purpose is to reveal the effect of the gradient parameters and the Poisson's ratio upon the half-plane's elastic response.

We begin with case (A) corresponding to a concentrated normal force P acted upon a traction-free half-plane (Fig. 1a). Figure 3 illustrates the variation of the normalized tangential $\overline{u}_x^{(P)}$ and normal $\overline{u}_y^{(P)}$ surface ($y = 0$) displacements in strain-gradient elasticity and in the classical theory. In particular, Figs. 3a and 3b exhibit the effect of the Poisson's ratio ν upon the strain-gradient and the classical solutions. It is observed that the tangential displacement (Fig. 3a) becomes smooth at the point of application of the concentrated force whereas the classical solution is discontinuous. The gradient effects are dominant within the zone $|x| < 6\ell_2$, while outside this region the gradient solution converges

quickly to the classical one. It is worth noting that when the material becomes incompressible, $\nu \to 0.5$ (green line in Fig. 3a), a reversal in the sign of the surface tangential displacement is observed very close to the point of application of the load. On the other hand, as it can be seen from Fig. 3b, the surface normal displacement becomes bounded and continuous at the origin. The gradient effects, however, are not so pronounced as for the tangential displacement being significant only in the narrow zone $|x| < 2\ell_2$.

Further, Figs 3c-3h illustrate the effects of the gradient parameters (d_0, d_1, d_2) on the surface displacements for a material with Poisson's ratio $\nu = 0.3$. The goal here is to highlight the possible deviations from the simplified gradient elasticity solution ($d_0 = d_1 = d_2 = 1$) when the complete Toupin-Mindlin theory is employed. To this purpose, in all Figures, two of the gradient parameters d_k are taken to be equal to unity while the third one varies spanning the range of positive definiteness as defined by Eqs (118) and (119). It is observed that the effect of the parameters d_0 and d_2 upon the solution is more significant than the effect of d_1. More specifically, it is shown that as the gradient parameter d_0 decreases, approaching the lower bound of (PD) ($d_0 \to 0$), the tangential and the normal surface displacements become significantly larger as compared to the simplified gradient theory (Figs 3c and 3d). Furthermore, a sign reversal is noticed in the values of the tangential displacement (black curve, Fig. 3c) very close to the point of application of the load. On the other hand, as the gradient parameter d_2 increases, approaching the upper bound of (PD) ($d_2 \to 3.03$), both surface displacements significantly decrease in magnitude (green curves, Figs 3g and 3h).

The variation of the surface strain components in strain-gradient elasticity for case (A) is displayed in Fig. 4 with respect to the Poisson's ratio and the gradient parameter d_1. It is noted that in classical elasticity all surface ($y = 0$) strain components are *null*. The simplified gradient elasticity case ($d_0 = d_1 = d_2 = 1$) is also depicted for comparison by a dash-dot (blue) line in Figs 4b, 4d, and 4f. It is remarkable that, in all cases, the strain components are *bounded* at the point of application of the concentrated force. The gradient effects are significant in the range $|x| < 10\ell_2$, outside this zone the surface strains tend to zero approaching the classical elasticity solution. In more detail, the distribution of the normalized surface strain $\bar{\varepsilon}_{xx}^{(P)}$ is depicted in Figs 4a and 4b. It is observed that as the Poisson's ratio increases approaching incompressibility, $\bar{\varepsilon}_{xx}^{(P)}$ changes from compressive to tensile (Fig. 4a). Furthermore, as d_1 increases, approaching the upper bound of (PD) ($d_1 \to 1.63$), $\bar{\varepsilon}_{xx}^{(P)}$ increases

significantly in a narrow region $|x| < 2\ell_2$ below the concentrated force (green curve – Fig. 4b). Similar observations hold for the strain component $\overline{\varepsilon}_{yy}^{(P)}$ (Figs 4c and 4d). Finally, it is shown that the shear strain $\overline{\varepsilon}_{xy}^{(P)}$ exhibits a bounded maximum at a distance $|x| = \ell_2$ from the origin and then quickly diminishes to zero approaching the classical null solution (Figs 4e and 4f).

A further comparison of the strain components in classical elasticity and in strain gradient elasticity can be seen in the contour plots presented in Fig. 5. It is noted that the full field solutions ($y > 0$) for the strain components have been obtained by numerically inverting the pertinent Fourier transforms. It is clearly observed that, contrary to the classical case, the strain gradient solution is bounded at the point of application of the concentrated vertical force. As we move away from the origin, the iso-contours of strain gradient theory converge to the classical ones.

Next, we examine case (B) corresponding to a concentrated tangential force S acting on the surface of the traction-free half-plane (Fig. 1b). In particular, Fig. 6 depicts the variation of the normalized tangential surface displacement $\overline{u}_x^{(S)}$ in strain-gradient elasticity and in the classical theory. The vertical normalized displacement $\overline{u}_y^{(S)}$ is not shown here since, according to Betti's reciprocal theorem (see section 4.2), is equal to $\overline{u}_x^{(P)}$ (Fig. 3). Contrary to the classical elasticity case, the tangential displacement becomes bounded and continuous at the point of application of the load.

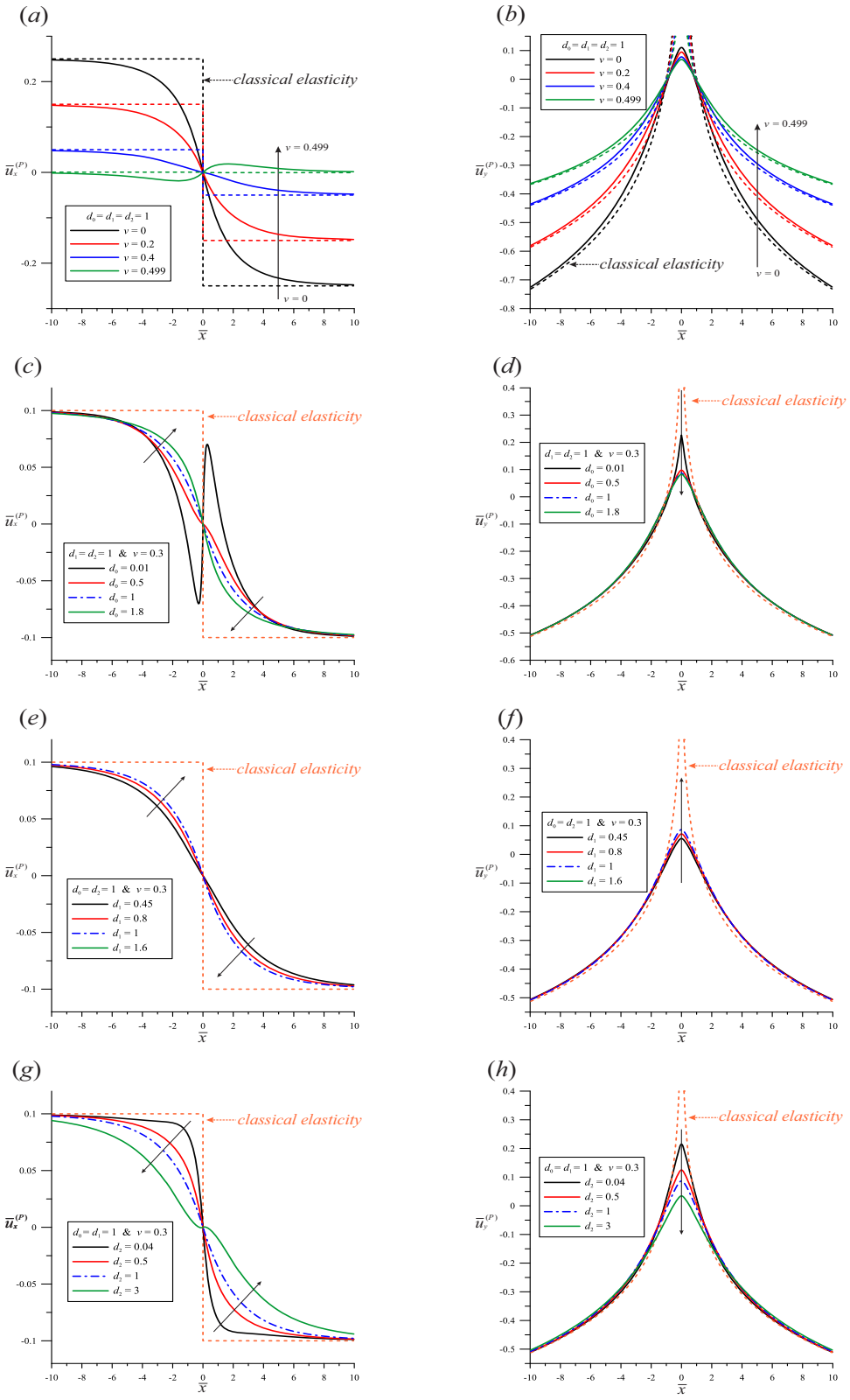

Figure 3: Normalized tangential and vertical surface displacements $\overline{u}_x^{(P)}$ and $\overline{u}_y^{(P)}$ for the case of the normal concentrated force P. The effects of the Poisson's ratio ν and of the gradient parameters d_0, d_1, d_2 are presented.

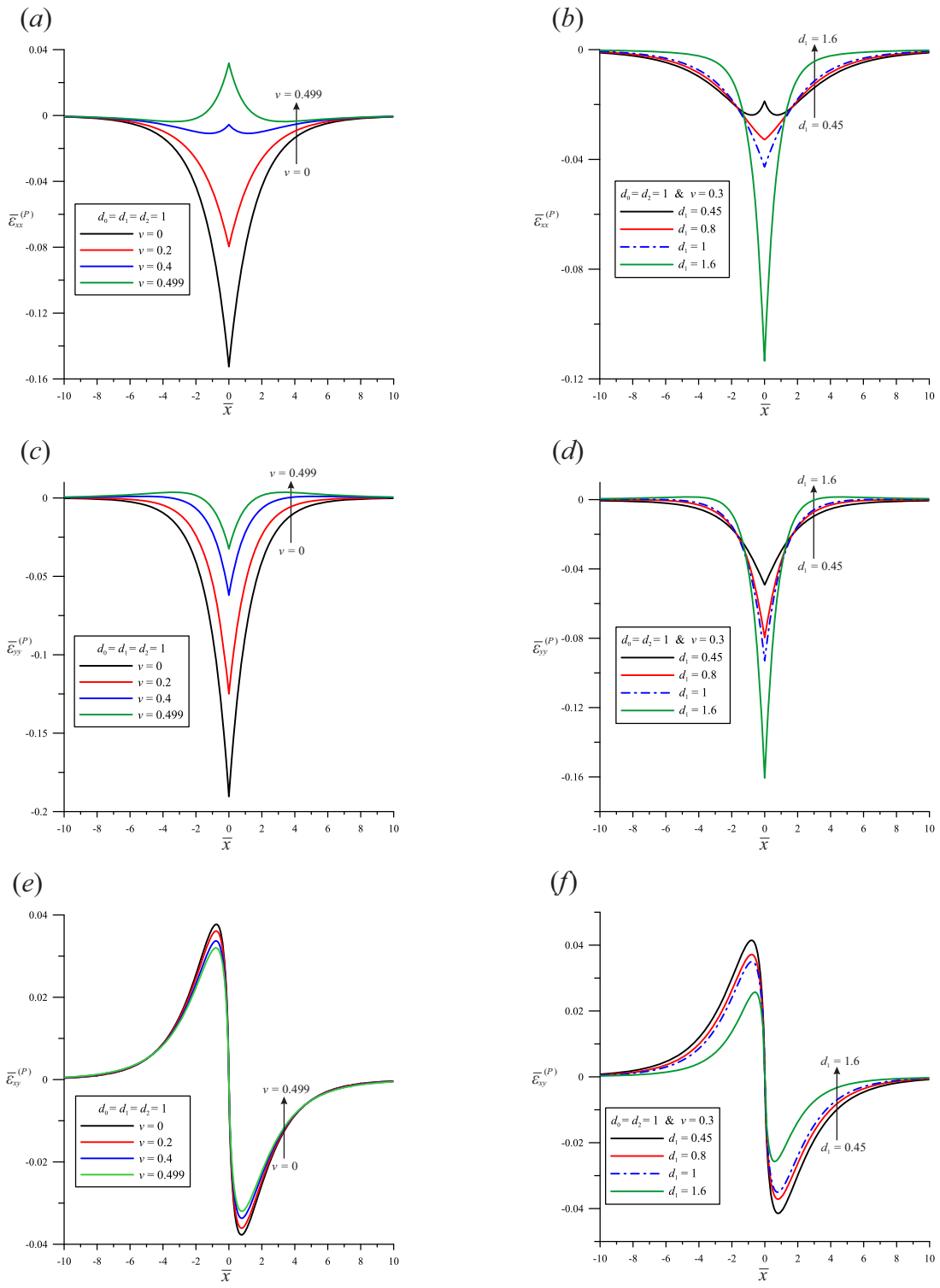

Figure 4: Normalized surface strain components $\left(\overline{\varepsilon}_{xx}^{(P)},\ \overline{\varepsilon}_{yy}^{(P)},\ \overline{\varepsilon}_{xy}^{(P)}\right)$ for the case of the normal concentrated load P. The effects of the Poisson's ratio ν and of the gradient parameter d_1 are presented.

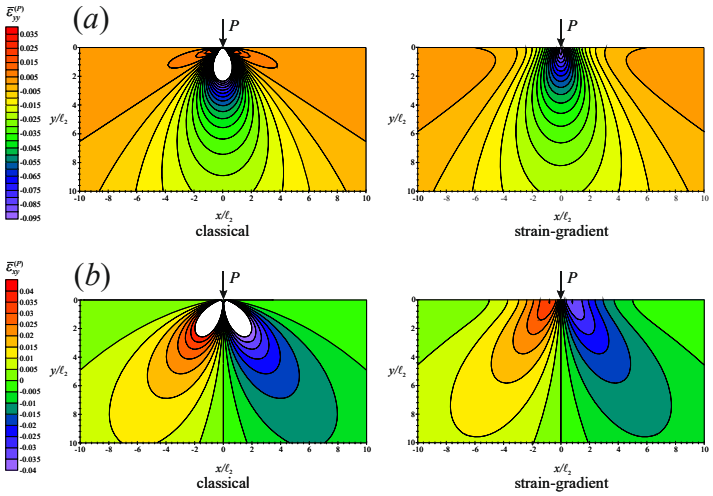

Figure 5: Iso-contours of normalized strain components (a) $\overline{\varepsilon}_{yy}^{(P)}$ and (b) $\overline{\varepsilon}_{xy}^{(P)}$, for the case of the normal concentrated load P. Results are shown for the cases of classical and simplified strain gradient elasticity ($d_0 = d_1 = d_2 = 1$).

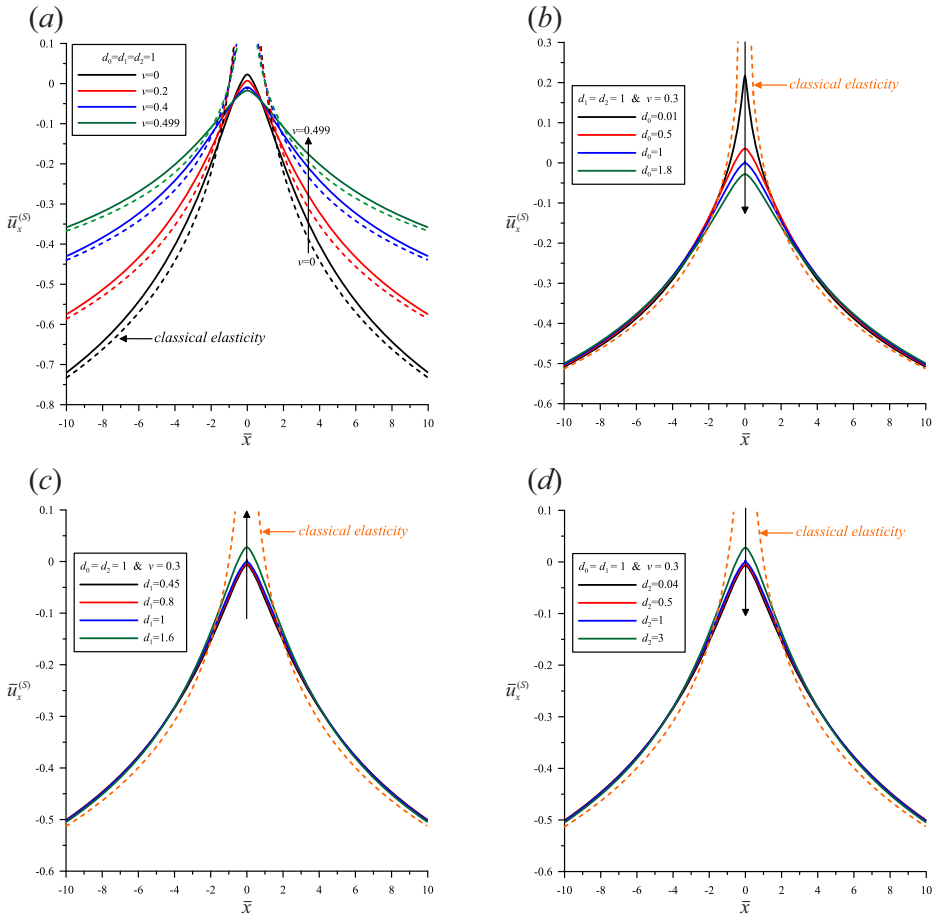

Figure 6: Normalized tangential surface displacement $\overline{u}_x^{(S)}$ for the case of the tangential concentrated force S. The effects of the Poisson's ratio ν and of the gradient parameters d_0, d_1, d_2 are presented.

Furthermore, the results for the displacement field in the cases (C)-(F), corresponding to a half-plane loaded by concentrated dipole forces with moments and without moments are shown in Fig. 7-14, at the surface of the half-plane as well as inside the half-plane in terms of contour plots. The effects of the Poisson's ratio ν and of the gradient parameters d_0, d_1, d_2 are highlighted. As previously, the values of the gradient parameters d_k span the range of positive definiteness. It is observed that for all cases the displacement field is bounded at the point of application of the concentrated dipole force.

In particular, for case (C) (Fig. 1c), corresponding to a dipole force M with moment in the *x*-direction, Fig. 7 shows that as d_0 decreases approaching the lower bound of (PD), keeping all the other parameters fixed, the normal displacement changes sign in the region of the application of the load. A similar observation holds for d_2 but the effect is then less significant. The full field solution for the displacement field is shown in terms of contours in Fig. 8 for the case of the simplified gradient elasticity.

The results for case (D) (Fig. 1d), corresponding to a dipole force T in the *y*-direction, are shown in Figs. 9 and 10. This type of loading does not produce a resultant force or moment. For this reason, the solution decays much faster than the one in case (C). This is clearly illustrated in Fig. 10 where the two components of the displacement field are shown in terms of contours for the case of the simplified gradient elasticity.

The results for case (E) regarding a dipole force Q with moment in the *y*-direction (Fig. 1e) are shown in Figs. 11 and 12. In this case, the classical elasticity solution suggests *null* tangential surface displacement $\overline{u}_x$, a result which is in marked contrast with the gradient solution. Indeed, as it can be seen from Fig. 11, the variation of the d_0 and d_1 parameters alter significantly the behavior of the tangential surface displacement not only quantitatively but also qualitatively. Moreover, contrary to the classical elasticity result, $\overline{u}_y$ is bounded but is moderately affected by the variation of the gradient parameters d_k.

Finally, the results for case (F) regarding the application of concentrated dipole force without moment in the *x*-direction (Fig. 1f) are shown in Figs. 13 and 14. Only the tangential displacement is shown here since, according to Betti's reciprocal theorem (see section 4.2), the normal displacement $\overline{u}_y^{(N)}$ in this case is equal to $\overline{u}_x^{(Q)}$ (Fig. 11). Contrary to the classical elasticity case, the tangential displacement becomes bounded and continuous at the point of application of the load.

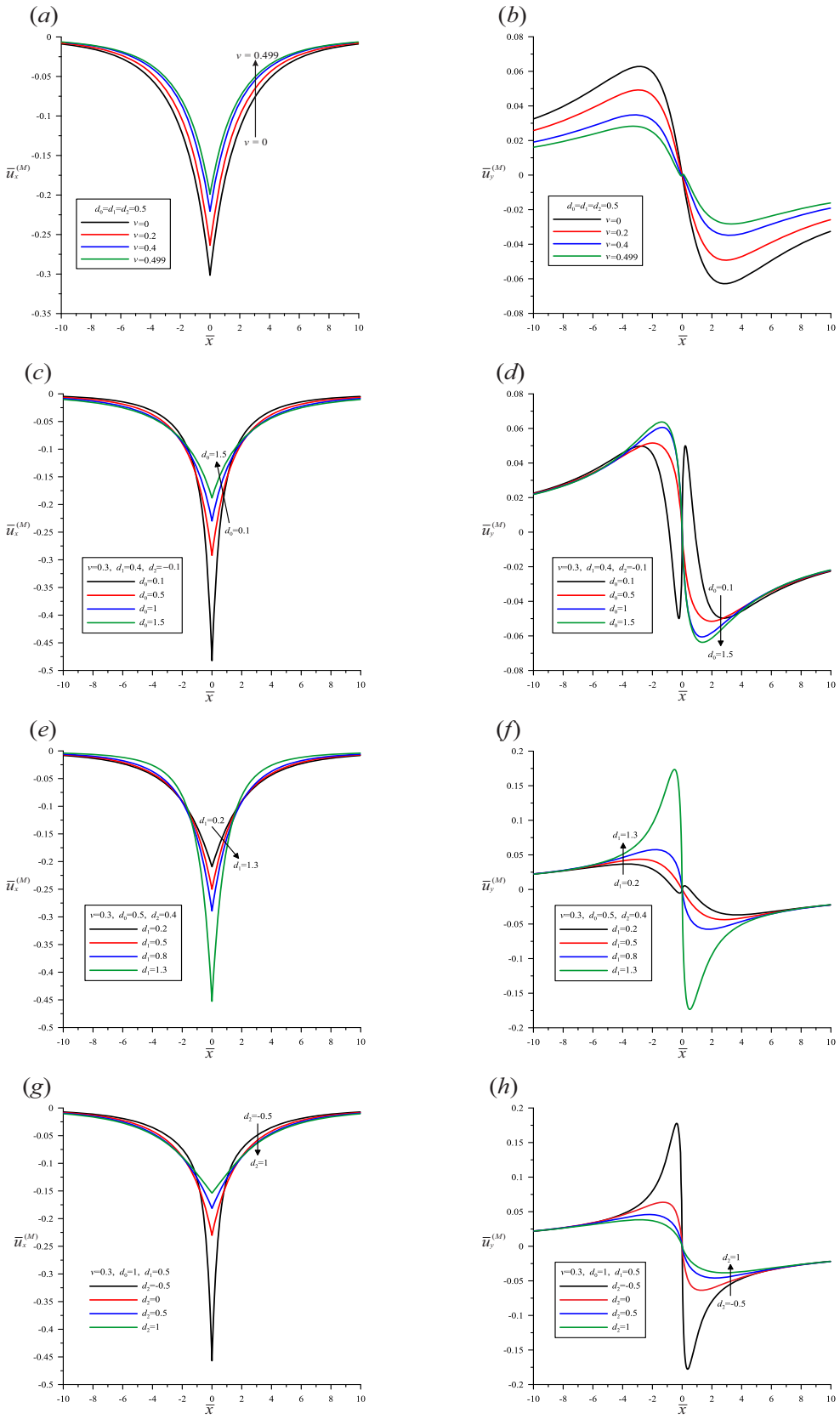

Figure 7: Normalized tangential and normal surface displacements $\overline{u}_x^{(M)}$ and $\overline{u}_y^{(M)}$ for the case of a dipole force with moment M in the *x*-direction. The effects of the Poisson's ratio ν and of the gradient parameters d_0, d_1, d_2 are presented.

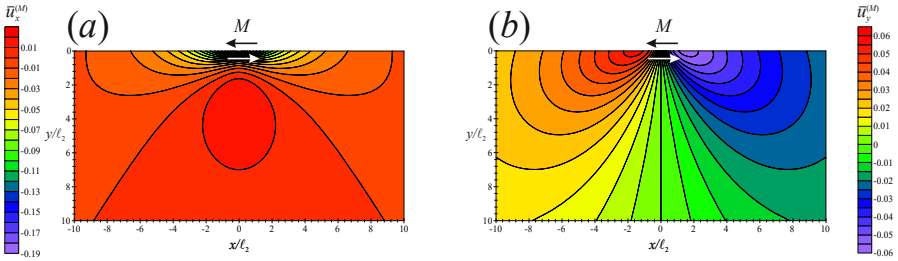

Figure 8: Iso-contours of normalized displacement components (a) $\overline{u}_x^{(M)}$ and (b) $\overline{u}_y^{(M)}$, due to a dipole force with moment M in the x-direction ($d_0 = d_1 = d_2 = 1$ and $\nu = 0.3$).

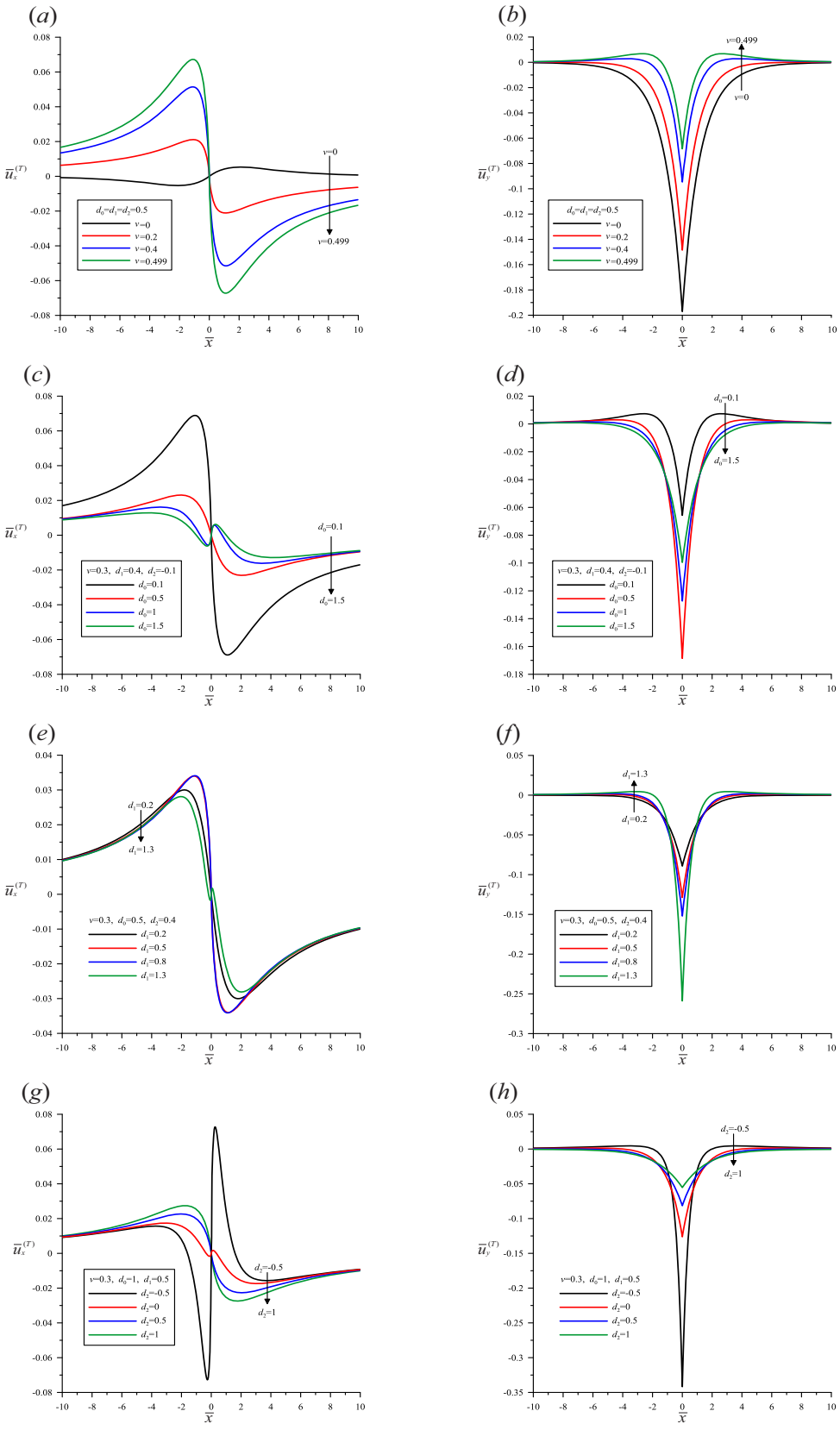

Figure 9: Normalized tangential and normal surface displacements $\overline{u}_x^{(T)}$ and $\overline{u}_y^{(T)}$ for the case of a dipole force without moment T. The effects of the Poisson's ratio ν and of the gradient parameters d_0, d_1, d_2 are presented.

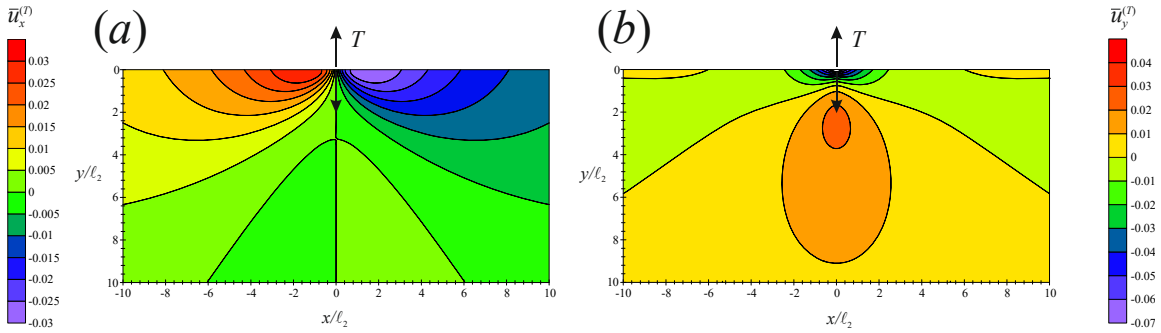

Figure 10: Iso-contours of normalized displacement components (a) $\overline{u}_x^{(T)}$ and $\overline{u}_y^{(T)}$ (b), for the case of the dipole force without moment T ($d_0 = d_1 = d_2 = 1$ and $\nu = 0.3$).

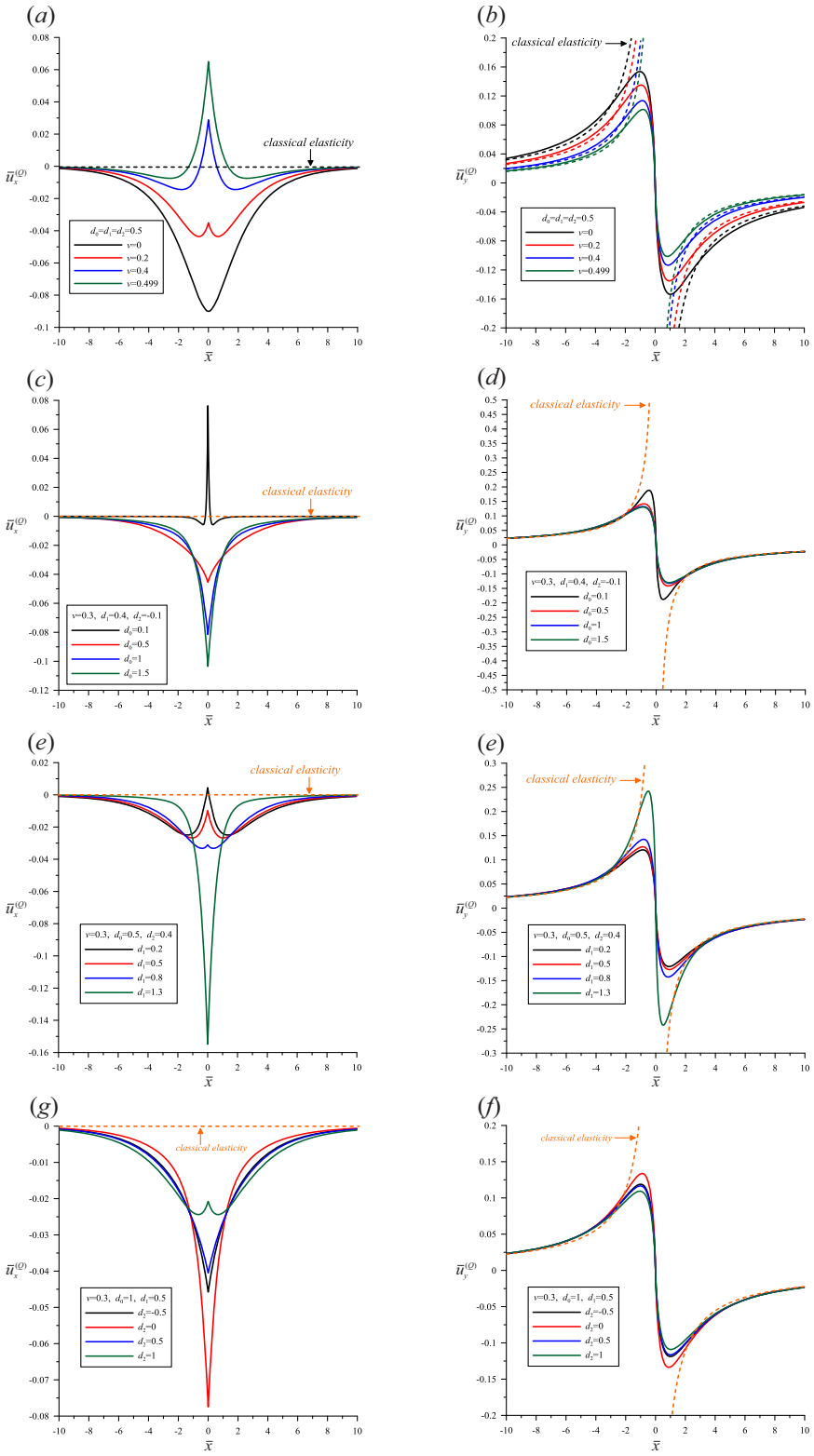

Figure 11: Normalized tangential and normal surface displacements $\bar{u}_x^{(Q)}$ and $\bar{u}_y^{(Q)}$ for the case of a dipole force Q with moment. The effects of the Poisson's ratio ν and of the gradient parameters d_0, d_1, d_2 are presented.

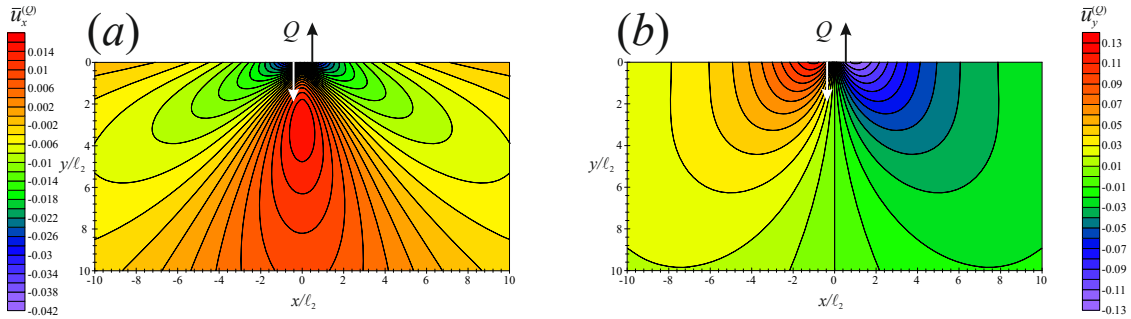

Figure 12: Iso-contours of normalized displacement components (a) $\bar{u}_x^{(Q)}$ and $\bar{u}_y^{(Q)}$ (b), for the case of a dipole force Q with moment ($d_0 = d_1 = d_2 = 1$ and $\nu = 0.3$).

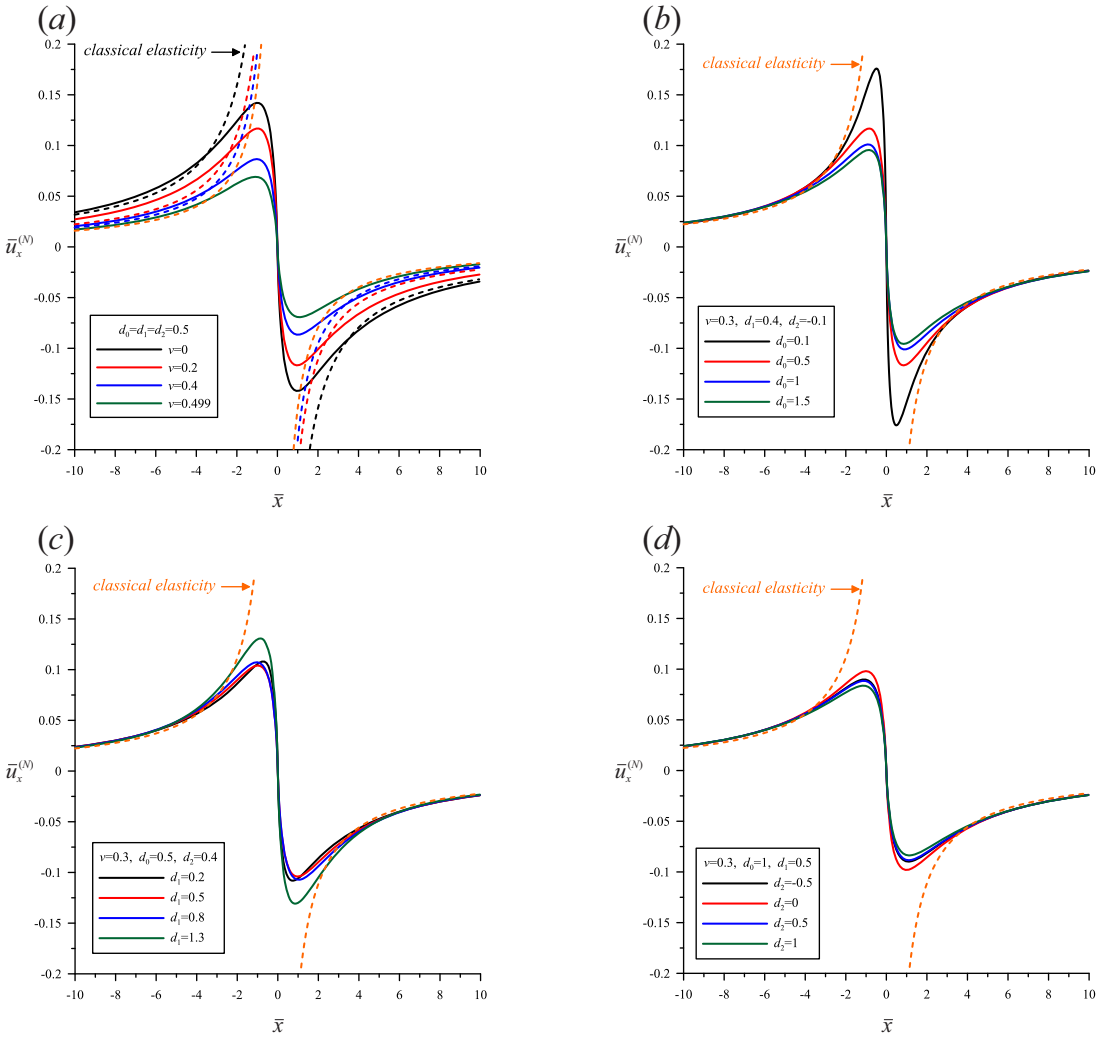

Figure 13: Normalized tangential and normal surface displacements $\bar{u}_x^{(N)}$ and $\bar{u}_y^{(N)}$ for the case of a dipole force N without moment. The effects of the Poisson's ratio ν and of the gradient parameters d_0, d_1, d_2 are presented.

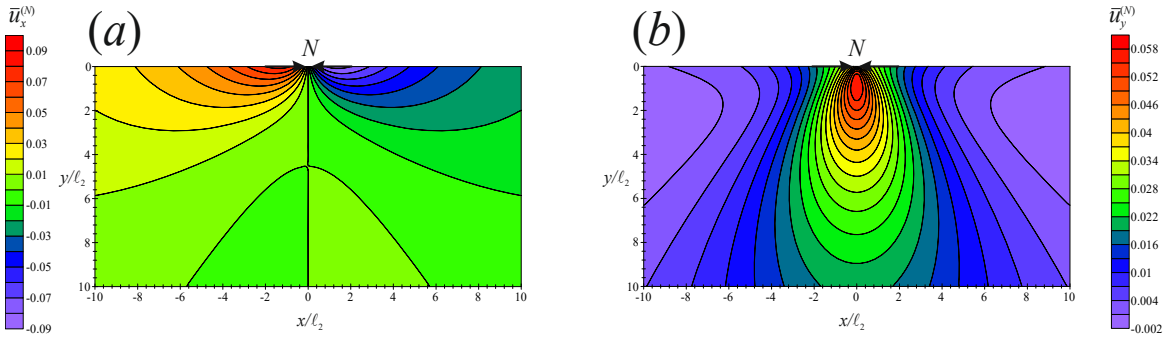

Figure 14: Iso-contours of normalized displacement components: (a) $\bar{u}_x^{(N)}$ and $\bar{u}_y^{(N)}$ (b) for the case of a dipole force N without moment ($d_0 = d_1 = d_2 = 1$ and $\nu = 0.3$).

7. Conclusions

In the present work, the Green's functions for various concentrated load half-plane problems were derived in the context of the complete Toupin-Mindlin theory of isotropic strain-gradient elasticity. An isotropic material in this framework is characterized by the two Lamé constants and additionally five strain-gradient parameters. Our main concern here was to determine possible deviations from the predictions of classical theory of elasticity but also from the simplified strain-gradient theory (involving only one gradient parameter) that is extensively used nowadays for the solution of boundary value problems.

The solution method is based on integral transforms and is exact. Of special importance is the behavior of the new solutions near to the point of application of the loads where pathological singularities and discontinuities exist in the classical solutions. In marked contrast with the predictions of classical elasticity, our results show that, in all cases, the displacement components are bounded and continuous at the points of application of the concentrated loads. This may have important implications for more general contact problems and the Boundary Element Method. For the Flamant problem, it was additionally shown that the strain field is also bounded which implies a finite energy contained within any finite portion of the body. Such a behavior seems to be more natural than the singular behavior present in the classical solutions. The use of the complete Toupin-Mindlin theory revealed interesting solution behaviors that cannot be captured by the simplified strain-gradient elasticity theory. Finally, we notice that an analytical solution such as the present one has an advantage over numerical solutions, especially in new areas of research where benchmark solutions do not exist.

References

Adler, W.F., 1969. Point-defect interactions in elastic materials of grade 2. *Physical Review* **186**, 666-674.

Anagnostou, D.S., Gourgiotis, P.A., Georgiadis, H.G., 2013. The Cerruti problem in dipolar gradient elasticity. *Mathematics and Mechanics of Solids* **20**, 1088-1106.

Anderson, W., Lakes, R., 1994. Size effects due to Cosserat elasticity and surface damage in closed-cell polymethacrylimide foam. *Journal of Materials Science* **29**, 6413-6419.

Agiasofitou, E.K., Lazar, M., 2009. Conservation and balance laws in linear elasticity of grade three. *Journal of Elasticity* **94**, 69-85.

Aravas, N., Giannakopoulos, A.E., 2009. Plane asymptotic crack-tip solutions in gradient elasticity. *International Journal of Solids and Structures* **46**, 4478-4503.

Bacca, M., Bigoni, D., Dal Corso, F., Veber, D., 2013. Mindlin second-gradient elastic properties from dilute two-phase Cauchy-elastic composites Part II: Higher-order constitutive properties and application cases. *International Journal of Solids and Structures* **50**, 4020-4029.

Barber, J.R., 1992. Elasticity. Springer.

Bigoni, D., Gourgiotis, P.A., 2016. Folding and faulting of an elastic continuum. *Proceedings of the Royal Society A* **472**, 20160018.

Bleustein, J.L., 1967. A note on the boundary conditions of Toupin's strain-gradient theory. *International Journal of Solids and Structures* **3**, 1053-1057.

Charalambopoulos, A., Polyzos, D., 2015. Plane strain gradient elastic rectangle in tension. *Archive of Applied Mechanics* **85**, 1421-1438.

Cook, T.S., Weitsman, Y., 1966. Strain-gradient effects around spherical inclusions and cavities. *International Journal of Solids and Structures* **2**, 393-406.

Cowin, S.C., 1969. Singular stress concentrations in plane Cosserat elasticity. *Zeitschrift für angewandte Mathematik und Physik* **20**, 979-982.

Day, F.D., Weitman, Y., 1966. Strain-gradient effects in microlayers. *ASCE Journal of Engineering Mechanics* **92**, 67-86.

Dyszlewicz, J., Matysiak, S., 1973. Singularity stresses in a micropolar elastic semi-space due to concentrated load. *Academie Polonaise des Sciences, Bulletin, Serie des Sciences Techniques* **21**, 469.

Eringen, A.C., Suhubi, E.S., 1975. Elastodynamics, Vol. 2. Academic Press, New York.

Eshel, N., Rosenfeld, G., 1973. Some two-dimensional exterior problems in a linear elastic solid of grade two. *Zeitschrift für Angewandte Mathematik und Mechanik* **53**, 761-772.

Eshel, N.N., Rosenfeld, G., 1970. Effects of strain-gradient on the stress-concentration at a cylindrical hole in a field of uniaxial tension. *Journal of Engineering Mathematics* **4**, 97-111.

Eshel, N.N., Rosenfeld, G., 1975. Axi-symmetric problems in elastic materials of grade two. *Journal of the Franklin Institute* **299**, 43-51.

Exadaktylos, G., 1999. Some basic half-plane problems of the cohesive elasticity theory with surface energy. *Acta Mechanica* **133**, 175-198.

Filopoulos, S., Papathanasiou, T.K., Markolefas, S.I., Tsamasphyros, G.J., 2010. Dynamic finite element analysis of a gradient elastic bar with micro-inertia. *Computational Mechanics* **45**, 311-319.

Gao, X.-L., Ma, H., 2009. Green's function and Eshelby's tensor based on a simplified strain gradient elasticity theory. *Acta Mechanica* **207**, 163-181.

Gao, X.-L., Zhou, S.-S., 2013. Strain gradient solutions of half-space and half-plane contact problems. *Zeitschrift für angewandte Mathematik und Physik* **64**, 1363-1386.

Georgiadis, H.G., Gourgiotis, P.A., Anagnostou, D.S., 2014. The Boussinesq problem in dipolar gradient elasticity. *Archive of Applied Mechanics* **84**, 1373-1391.

Georgiadis, H.G., Vardoulakis, I., Lykotrafitis, G., 2000. Torsional surface waves in a gradient-elastic half-space. *Wave Motion* **31**, 333-348.

Georgiadis, H.G., Anagnostou, D.S., 2008. Problems of the Flamant–Boussinesq and Kelvin type in dipolar gradient elasticity. *Journal of Elasticity* **90**, 71-98.

Georgiadis, H.G., Grentzelou, C.G., 2006. Energy theorems and the J-integral in dipolar gradient elasticity. *International journal of Solids and Structures* **43**, 5690-5712.

Georgiadis, H.G., Vardoulakis, I., Velgaki, E.G., 2004. Dispersive Rayleigh-wave propagation in microstructured solids characterized by dipolar gradient elasticity. *Journal of Elasticity* **74**, 17-45.

Goryacheva, I.G., 2013. Contact mechanics in tribology. Springer Science & Business Media.

Gourgiotis, P.A., Georgiadis, H.G., 2009. Plane-strain crack problems in microstructured solids governed by dipolar gradient elasticity. *Journal of the Mechanics and Physics of Solids* **57**, 1898-1920.

Gourgiotis, P.A., Sifnaiou, M.S., Georgiadis, H.G., 2010. The problem of sharp notch in microstructured solids governed by dipolar gradient elasticity. *International Journal of Fracture* **166**, 179-201.

Gourgiotis, P.A., Georgiadis, H.G., 2015. Torsional and SH surface waves in an isotropic and homogenous elastic half-space characterized by the Toupin-Mindlin gradient theory. *International Journal of Solids and Structures* **62**, 217-228.

Green, A.E., Naghdi, P.M., 1968. A note on simple dipolar stresses. *Journal de Mecanique* **7**, 465-474.

Grentzelou, C.G., Georgiadis, H.G., 2005. Uniqueness for plane crack problems in dipolar gradient elasticity and in couple-stress elasticity. *International Journal of Solids and Structures* **42**, 6226-6244.

Grentzelou, C.G., Georgiadis, H.G., 2008. Balance laws and energy release rates for cracks in dipolar gradient elasticity. *International Journal of Solids and Structures* **45**, 551-567.

Hazen, G., Weitsman, Y., 1968. Stress concentration in strain-gradient bodies. *ASCE Journal of Engineering Mechanics* **94**, 773-795.

Jaunzemis, W., 1967. Continuum mechanics. Macmillan, New York.

Johnson, K.L., 1987. Contact mechanics. Cambridge University Press.

Lardner, R., 1970. Singular stress concentrations in second-grade materials. *Quarterly of Applied Mathematics* **28,** 111-121.

Lardner, R., 1971. Dislocations in materials with couple stress. *IMA Journal of Applied Mathematics* **7**, 126-137.

Lazar, M., Maugin, G.A., 2006. A note on line forces in gradient elasticity. *Mechanics Research Communications* **33**, 674-680.

Lazar, M., 2016. Irreducible decomposition of strain gradient tensor in isotropic strain gradient elasticity. *Zeitschrift für Angewandte Mathematik und Mechanik* **96**, 1291-1305.

Li, Y., Wei, P., 2015. Reflection and transmission of plane waves at the interface between two different dipolar gradient elastic half-spaces. *International Journal of Solids and Structures* **56**, 194-208.

Love, A.E.H., 1944. A treatise on mathematical theory of elasticity. Dover, New York.

Mindlin, R.D., 1964. Micro-structure in linear elasticity. *Archive for Rational Mechanics and Analysis* **16**, 51-78.

Mindlin, R.D., Eshel, N.N., 1968. On first strain-gradient theories in linear elasticity. *International Journal of Solids and Structures* **4**, 109-124.

Muki, R., Sternberg, E., 1965. The influence of couple-stresses on singular stress concentrations in elastic solids. *Zeitschrift für angewandte Mathematik und Physik* **16**, 611-648.

Nowinski, J., 1986. The Boussinesq-Flamant problem for an elastic nonlocal half-infinite space. *Acta Mechanica* **58**, 59-66.

Papargyri-Beskou, S., Tsepoura, K., Polyzos, D., Beskos, D.E, 2003. Bending and stability analysis of gradient elastic beams. *International Journal of Solids and Structures* **40**, 385-400.

Papathanasiou, T.K., Gourgiotis, P.A., Dal Corso, F., 2016. Finite element simulation of a gradient elastic half-space subjected to thermal shock on the boundary. *Applied Mathematical Modelling* 40, 10181-10198.

Po, G., Lazar, M., Admal, N. C., Ghoniem, N., 2017. A non-singular theory of dislocations in anisotropic crystals. *arXiv preprint* arXiv:1706.00828.

Podio-Guidugli, P., Favata, A., 2014. Elasticity for geotechnicians. Springer.

Polyzos, D., Tsepoura, K.G., Tsinopoulos, S.V., Beskos, D.E., 2003. A boundary element method for solving 2-D and 3-D static gradient elastic problems. Part I: Integral formulation. *Computer Methods in Applied Mechanics and Engineering* **192**, 2845-2873.

Reda, H., Goda, I., Ganghoffer, J., L'Hostis, G., Lakiss, H., 2017. Dynamical analysis of homogenized second gradient anisotropic media for textile composite structures and analysis of size effects. *Composite Structures* 161, 540-551.

Roos, B.W., 1969. Analytic functions and distributions in physics and engineering. Wiley, New York.

Rosi, G., Nguyen, V.-H., Naili, S., 2014. Reflection of acoustic wave at the interface of a fluid-loaded dipolar gradient elastic half-space. *Mechanics Research Communications* **56**, 98-103.

Rosi, G., Auffray, N., 2016. Anisotropic and dispersive wave propagation within strain-gradient framework. *Wave Motion* 63, 120-134.

Sciarra, G., Vidoli, S., 2012. The role of edge forces in conservation laws and energy release rates of strain-gradient solids. *Mathematics and Mechanics of Solids* **17**, 266-278.

Sciarra, G., Vidoli, S., 2013. Asymptotic fracture modes in strain-gradient elasticity: size effects and characteristic lengths for isotropic materials. *Journal of Elasticity* **113**, 27-53.

Shodja, H.M., Zaheri, A., Tehranchi, A., 2013. Ab initio calculations of characteristic lengths of crystalline materials in first strain gradient elasticity. *Mechanics of Materials* **61**, 73-78.

Sneddon, I.N., 1975. Application of integral transforms in the theory of elasticity. Springer-Verlag, New York.

Sternberg, E., 1960. On the integration of the equations of motion in the classical theory of elasticity. *Archive for Rational Mechanics and Analysis* **6**, 34-50.

Timoshenko, S.P., Woinowsky-Krieger, S., 1959. Theory of plates and shells. Mc Graw-Hill, New York.

Timoshenko, S.P., 1970. Theory of Elasticity. Mc Graw Hill, New York.

Toupin, R.A., 1962. Elastic materials with couple-stresses. *Archive for Rational Mechanics and Analysis* **11**, 385-414.

Turteltaub, M., Sternberg, E., 1968. On concentrated loads and Green's functions in elastostatics. *Archive for Rational Mechanics and Analysis* **29**, 193-240.

Vardoulakis, I., Georgiadis, H.G., 1997. SH surface waves in a homogeneous gradient-elastic half-space with surface energy. *Journal of Elasticity* **47**, 147-165.

Vardoulakis, I., Giannakopoulos, A., 2006. An example of double forces taken from structural analysis. *International Journal of Solids and Structures* **43**, 4047-4062.

Wang, R., 1990. A Line-force loading on the surface of a nonlocal elastic half-infinite medium. *International Journal of Solids and Structures* **26**, 1305-1311.

Weitsman, Y., 1966. Strain-gradient effects around cylindrical inclusions and cavities in a field of cylindrically symmetric tension. *Journal of Applied Mechanics* **33**, 57-67.